16. ICE IN THE MARTIAN REGOLITH

S. W. SQUYRES
Cornell University

S. M. CLIFFORD
Lunar and Planetary Institute

R. O. KUZMIN
V.I.Vernadsky Institute

J. R. ZIMBELMAN
Smithsonian Institution

and

F. M. COSTARD
Laboratoire de Géographie Physique

Geologic evidence indicates that the Martian surface has been substantially modified by the action of liquid water, and that much of that water still resides beneath the surface as ground ice. The pore volume of the Martian regolith is substantial, and a large amount of this volume can be expected to be at temperatures cold enough for ice to be present. Calculations of the thermodynamic stability of ground ice on Mars suggest that it can exist very close to the surface at high latitudes, but can persist only at substantial depths near the equator. Impact craters with distinctive lobate ejecta deposits are common on Mars. These rampart craters apparently owe their morphology to fluidization of subsurface materials, perhaps by the melting of ground ice, during impact events. If this interpretation is correct, then the size-frequency distribution of rampart

craters is broadly consistent with the depth distribution of ice inferred from stability calculations. A variety of observed Martian landforms can be attributed to creep of the Martian regolith abetted by deformation of ground ice. Global mapping of creep features also supports the idea that ice is present in near-surface materials at latitudes higher than ± 30°, and suggests that ice is largely absent from such materials at lower latitudes. Other morphologic features on Mars that may result from the present or former existence of ground ice include chaotic terrain, thermokarst and patterned ground.

One of the most significant realizations to come from the exploration of Mars has been that a very important role has been played in the planet's history by water and ice. Many of Mars' major geologic features, particularly the spectacular channels, appear to have formed by release of water from beneath the ground. Large amounts of water were involved in forming these and other features, and there is no obvious way that so much water could have been lost from the planet since they developed. It is commonly concluded, therefore, that a significant quantity of water resides on Mars, locked up beneath the surface as ground ice. Ground ice is the largest prospective reservoir for Martian H_2O, and if we can determine the total amount of H_2O present as ground ice, we will have learned much about the planet's total water inventory. As we discuss below, the presence of ground ice appears to have had significant effects on the morphology of surface features. And, if we are ever to send humans to Mars, ground ice may present one of the best hopes for finding a water resource on the planet. In this chapter, we outline the physical mechanisms that control the distribution of ice in the Martian regolith, and discuss the geologic features that provide evidence concerning this distribution.

I. THE MARTIAN MEGAREGOLITH

Impact processes have played a major role in the structural evolution of the Martian crust (Soderblom et al. 1974; Gumis 1981). Field studies of terrestrial impact craters (Shoemaker 1963; Short 1970; Dence et al. 1977) and theoretical models of the cratering process (Melosh 1980*a*; O'Keefe and Ahrens 1981) have shown that impacts modify a planetary surface by the production and dispersal of large quantities of ejecta, and through the intense fracturing of the surrounding and underlying basement. Fanale (1976) has estimated that over the course of Martian geologic history, the volume of ejecta produced by impacts was sufficient to have created a global blanket of debris up to 2 km thick. As noted by Carr (1979), it is likely that this ejecta layer is discontinuously interbedded with volcanic flows, weathering products, and sedimentary deposits, all overlying a heavily fractured basement (Fig. 1). This description of the near-surface structure of the Martian crust is very similar to that proposed for the Moon (Hartmann 1973*a*,1980), where an early period of intense bombardment resulted in the production of a

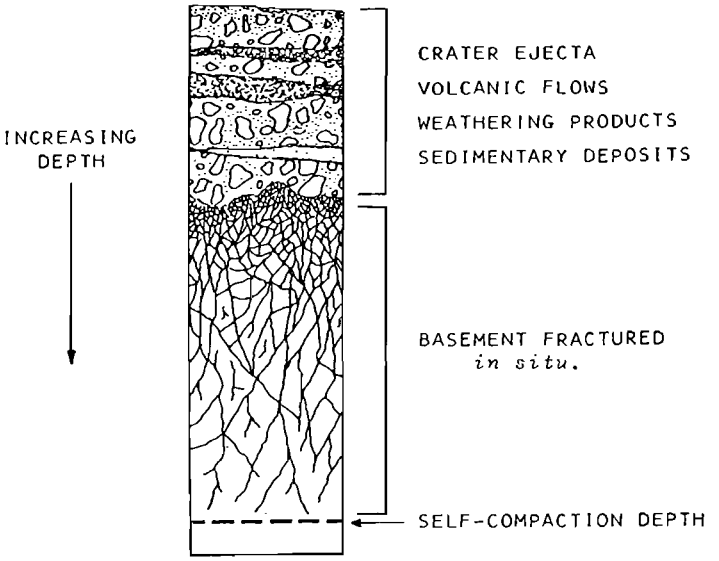

Fig. 1. An idealized stratigraphic column of the Martian crust (figure from Clifford 1981). The first km or so may consist of interbedded layers of different materials in a sequence which depends upon local geologic history.

blocky, porous megaregolith that extends to considerable depth—a view supported by the seismic propagation characteristics of the lunar crust (Toksöz 1979).

A. Porosity versus Depth

For the near surface of the Moon, seismic *P*-wave velocities increase with depth until they reach a local maximum at about 20 km (Toksöz 1979). This behavior is consistent with a reduction in crustal porosity with increasing depth, and hence lithostatic pressure. The transition between fractured and coherent lunar basement is believed to coincide with the beginning of a constant velocity zone (> 20 km), where lithostatic pressure is thought to be sufficient (> 1 kbar = 10^8 Pa) to close virtually all fracture and intergranular pore space (Toksöz 1979; Binder and Lange 1980).

Binder and Lange (1980) suggest that the seismic properties of the lunar crust are best explained by an exponential decline in porosity with depth. According to this model, the porosity at a depth z is given by

$$\Phi(z) = \Phi(0)\exp(-z/K) \tag{1}$$

where $\Phi(0)$ is the porosity at the lunar surface and K is a decay constant. Binder and Lange found that a porosity decay constant of 6.5 km best fit the lunar data. Assuming comparable crustal densities, the appropriate gravita-

tionally scaled value for Mars is 2.8 km, i.e., $K_{mars} = K_{moon}(g_{moon}/g_{mars})$ (Clifford 1981).

Two potential porosity profiles of the Martian crust are illustrated in Fig. 2. The first is based on a surface porosity of 20%, the same value assumed for the Moon by Binder and Lange (1980), and one that agrees reasonably well with the measured porosity of lunar breccias (Warren and Rasmussen 1987). This model yields a self-compaction depth (the depth at which crustal porosity becomes $< 1\%$, a value at which pore spaces typically become discontinuous) of approximately 8.5 km, and a total pore volume of roughly 8×10^7 km^3, a volume sufficient to store a global layer of water approximately 550 m deep (Clifford 1981,1984).

In the second profile, a surface porosity of 50% is assumed, a value consistent with estimates of the bulk porosity of Martian soil as analyzed by the Viking Landers (Clark et al. 1976). A surface porosity this large conceivably could be appropriate if the regolith has undergone a significant degree of weathering (see, e.g., Malin 1974; Huguenin 1976; Gooding 1978) or if it contains large segregated bodies of ground ice. The self-compaction depth predicted by this model is roughly 11 km, while its total pore volume is approximately 2×10^8 km^3, a volume equivalent to a global ocean some 1.4 km deep (Clifford 1984). It is doubtful, however, that weathering or large-scale ice segregation will affect more than the upper few km of the crust; therefore, below this depth, the porosity profile will most likely resemble the gravitationally scaled lunar curve.

The presence of groundwater could affect estimates of the self-compaction depth and total pore volume in several ways. As discussed by Hubert and Rubey (1959) and Byerlee and Brace (1968), the hydrostatic pressure of water within a pore can partially offset the lithostatic pressure acting to close it. For a "wet" Mars, crustal porosity may persist to depths roughly a third greater than those indicated by the "dry" models in Fig. 2. Ground-

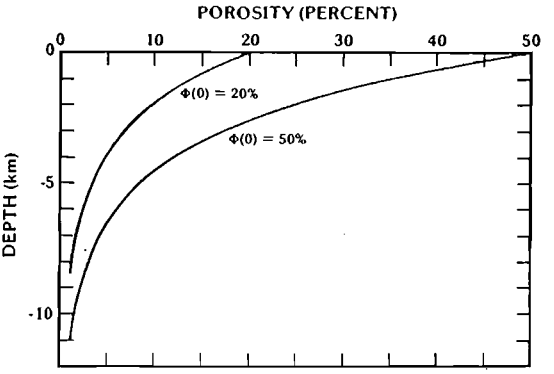

Fig. 2. Theoretical porosity profiles of the Martian crust based on a lunar analog (figure from Clifford 1981,1984).

water can also reduce crustal porosity by solution, compaction, and cementation (Maxwell 1964; Rittenhouse 1971). Such processes are of greatest significance under conditions of high temperature and pressure (Maxwell 1964; Pettijohn 1975). Currently these conditions are likely to exist only at great depth on Mars, where their impact on the overall porosity of the megaregolith is expected to be small. However, conditions were almost certainly different in the past. Models of the thermal history of Mars suggest that 4 Gyr ago the planet's internal heat flow and geothermal gradient were ~ 5 times larger than they are today (see chapter 5). In addition, an early greenhouse may have permitted liquid water to exist at or near the surface, where it may have reacted with atmospheric CO_2 to form carbonates within the crust (Kahn 1985; Postawko and Kuhn 1986; Pollack et al. 1987; see also chapter 32). The extent to which such processes have affected the porosity and depth of the megaregolith cannot be assessed.

B. Thermal Structure

The zone of permafrost on Mars is, like permafrost on Earth, defined as that portion of the crust where the temperature remains continuously below the freezing point of water. Because the term permafrost is so often misused, however, we instead adopt for this region the unambiguous term cryolithosphere, which is widely used in the Soviet literature (see, e.g., Kuzmin 1977). If we assume a solute-free freezing point of 273 K, then temperatures are below freezing at or immediately below the surface at every latitude, defining the cryolithosphere's upper bound. (While temperatures in the uppermost diurnal skin depth of Mars can exceed 273 K, this "active layer" of the Martian cryolithosphere is expected to be thoroughly desiccated.) The depth to the lower bound of the cryolithosphere is considerably less certain, because neither the magnitude of the Martian geothermal heat flux nor the thermal conductivity of the crust are known.

The depth z to the base of the cryolithosphere can be calculated from the steady-state one-dimensional heat conduction equation

$$z = k\frac{T_{mp} - T_{ms}}{Q_g} \tag{2}$$

where k is the thermal conductivity of the regolith, T_{ms} is the mean annual surface temperature, T_{mp} is the melting point temperature and Q_g is the value of the geothermal heat flux (Fanale 1976). At present, only the current latitudinal range of mean annual surface temperatures is known to any accuracy (~ 160 to 220 ± 5 K), while the remaining variables have associated uncertainties of 25 to 100%. Plausible ranges for each of these variables are discussed below.

Four principal factors influence the thermal conductivity of terrestrial permafrost: bulk density, degree of pore saturation, particle size and temper-

ature (Clifford and Fanale 1985). An increase in bulk density and/or pore saturation increases the thermal conductivity of permafrost because the conductivities of rock and ice are significantly higher than that of the air they displace. The effects of particle size and temperature are more complicated. Experiments have shown that thin films of adsorbed water remain unfrozen on silicate surfaces down to very low temperatures (Anderson et al. 1967; Anderson and Tice 1973), particularly in the presence of salts (Banin and Anderson 1974). Because the thermal conductivity of unfrozen water (~ 0.54 W m^{-1} K^{-1}; Penner 1970) is lower than that of ice, its presence will decrease the effective thermal conductivity of silicate-ice mixtures. As the quantity of H_2O adsorbed per unit surface area is roughly constant for all mineral soils, the conductivity of a frozen soil is related directly to its content of high specific surface-area clay; the effects on thermal conductivity of unfrozen water are generally seen only when a significant clay fraction is present. As the temperature of a frozen soil declines, so too does its content of adsorbed water. This results in an increase in the soil's effective conductivity, an increase that is compounded by the temperature dependence of the thermal conductivity of ice, which rises from 2.25 W m^{-1} K^{-1} at 273 K, to 4.42 W m^{-1} K^{-1} at 160 K (Ratcliffe 1962).

Remote thermal measurements at the two Viking landing sites indicate soil thermal conductivities in the range of 0.075 to 0.11 W m^{-1} K^{-1} (Kieffer 1976). However, in addition to the fine materials present, Viking Lander and Orbiter images also show that volcanics and other massive rocks make a significant contribution to the volume and mechanical properties of the outer portion of the Martian crust (see, e.g., Greeley and Spudis 1981). In light of this observation, it is important to note that terrestrial basalts typically have conductivities in the range of 1.5 to 3.5 W m^{-2} K^{-1} (Clifford and Fanale 1985). Given the range of possible variations in regolith composition and lithology, a thermal conductivity of 2 W m^{-1} K^{-1} ($\pm$ 1.0 W m^{-1} K^{-1}) appears to be a reasonable guess for the top few km of the Martian crust (Clifford and Fanale 1985).

Another factor that influences the depth to the base of the cryolithosphere is the melting temperature of the ice. The melting point can be depressed below 273 K by both pressure and solute effects. The effect of pressure is minor ($\sim 7.43 \times 10^{-8}$ K Pa^{-1}; Hobbs 1974), while the effect of dissolved salts can be quite large. The existence of various salts in the regolith is supported by the discovery of a duricrust layer at both Viking Lander sites and by the elemental composition of this duricrust as determined by the inorganic chemical analysis experiments on board each spacecraft (Toulmin et al. 1977; Clark 1978; Clark and Van Hart 1981). Among the most commonly cited candidate salts are NaCl, $MgCl_2$ and $CaCl_2$, which have associated freezing points (at their eutectic) of 252 K, 238 K and 218 K, respectively (Clark and Van Hart 1981). Multicomponent salt solutions can have eutectic

temperatures as low as 210 K (Brass 1980). Although the presence of $CaCl_2$ and $MgCl_2$ cannot be ruled out, serious questions have been raised concerning their chemical and thermodynamic stability under ambient Martian conditions, particularly in the presence of abundant sulfates (Clark and Van Hart 1981). Given these arguments, brines based on NaCl are probably the most likely candidates to be found on Mars.

Based on the assumption that Mars has the same K, U and Th concentrations as chondrites, Fanale (1976) has estimated a current geothermal heat flux on the order of 3×10^{-2} W m^{-2}. More detailed thermal modeling by Toksöz and Hsui (1978) and Davies and Arvidson (1981) has yielded the slightly higher estimates of 3.5×10^{-2} W m^{-2} and 4×10^{-2} W m^{-2}, respectively. As noted previously, the geothermal heat flow of Mars was probably much greater in the past—particularly during the planet's first half Gyr of geologic history, the period in which it was radiating away most of its accretional heat.

Substituting the best current estimates of Martian heat flow, crustal thermal conductivity, and melting temperature into Eq. (2), the depth to the base of the cryolithosphere is found to vary from 1 to 3 km at the equator to approximately 3 to 8 km at the poles (Fig. 3)—the poleward increase in depth reflecting the corresponding latitudinal decline in mean annual surface temperature (Fanale 1976; Rossbacher and Judson 1981; Crescenti 1984; Clifford 1984,1987*b*). By integrating the crustal porosity profile given by Eq. (1) down to the melting isotherm depths calculated from Eq. (2), the pore volume of the Martian cryolithosphere can be estimated. For the likely physical and thermal properties of the megaregolith, this amounts to a volume of 10^7 to 10^8 km^3. (Note that this volume is distinct from the *total* megaregolith pore volume calculated above.) The quantity of H_2O required to saturate this pore volume is equivalent to a global layer of water approximately 70 to 700 m deep (Clifford 1984,1987*b*).

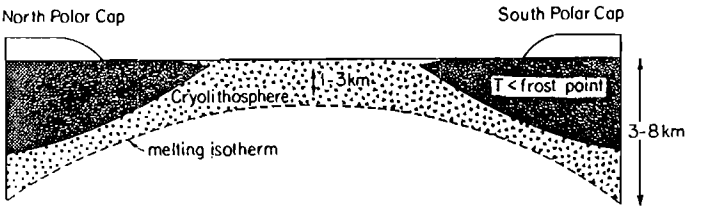

Fig. 3. A pole-to-pole cross section of the Martian crust illustrating the theoretical latitudinal variation in depth of the 273 K isotherm. Ground ice can exist in equilibrium with the atmosphere only at those latitudes and depths where crustal temperatures are below the frost point of atmospheric water vapor (~ 198 K; Farmer and Doms 1979). Outside these locations, ground ice can only survive if it is diffusively isolated from the atmosphere by a regolith of low gaseous permeability (see, e.g., Smoluchowski 1968; Clifford and Hillel 1983; Fanale et al. 1986) (Figure adapted from Fanale 1976 and Rossbacher and Judson 1981.)

C. Ground Ice Stability

Although mean annual surface temperatures are below freezing everywhere on Mars, observations made by the Viking Orbiter Mars Atmospheric Water Detectors (MAWD) indicate a global frost point temperature of roughly 200 K. As a result, the existence of ground ice in equilibrium with the water vapor content of the atmosphere is restricted to the colder latitudes poleward of about ± 40° (Farmer and Doms 1979).

Despite the current instability, there is a large body of morphologic evidence that suggests that ground ice has existed in the equatorial regolith throughout much of Martian geologic history (Carr and Schaber 1977; Mouginis-Mark 1979; Allen 1979; Rossbacher and Judson 1981; Squyres 1984; Carr 1986; Lucchitta 1987*c*). This evidence presents a problem, for it is difficult to account for both the initial origin and continued survival of ground ice in a region where the present mean annual temperature exceeds the frost point by more than 20 K. However, the problem may be resolved if equatorial ground ice is a relic of a former climate that has been preserved by the diffusion-limiting properties of a fine-grained regolith (Smoluchowski 1968; Kuzmin 1978; Clifford and Hillel 1983; Fanale et al. 1986).

The stability of equatorial ground ice is governed by the rate at which H_2O molecules can diffuse through the regolith and into the atmosphere. This process is complicated by the fact that the mean free path of an H_2O molecule in the Martian atmosphere is $\sim$ 10 μm. When the ratio of the pore radius r to the mean free path λ of the diffusing molecules is large ($r/\lambda > 10$), bulk molecular diffusion is the dominant mode of transport; the movement of molecules through the pore system occurs in response to repeated collisions with other molecules present in the pores. On the other hand, for very small pores ($r/\lambda < 0.1$), collisions between the diffusing molecules and the pore walls greatly outnumber those that occur with other molecules, leading to the process known as Knudsen diffusion. Because the frequency of pore wall collisions increases with decreasing pore size, small pores can substantially reduce the efficiency of the transport process. For pores of intermediate size ($0.1 < r/\lambda < 10$), the contributions of both processes must be taken into account. The effect is illustrated in Fig. 4, where the effective diffusion coefficient of H_2O is shown as a function of pore size.

The survival of equatorial ground ice was considered in detail by Clifford and Hillel (1983) and Fanale et al. (1986). They found that near the equator the regolith has probably been desiccated to a depth of several hundred m over the past 3.5 Gyr, assuming that our current knowledge of the quasi-periodic changes in Martian obliquity and orbital elements is accurate (Ward 1979; Toon et al. 1980; chapter 9). However, because the sublimation rate of H_2O is sensitively dependent on temperature, the amount of ice lost at higher latitudes is expected to be much less, falling to perhaps a few tens of m at 35° latitude (Fig. 5; see also chapter 33). Greater depths of desiccation might

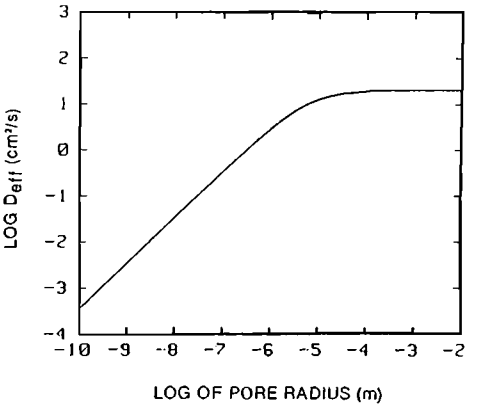

Fig. 4. A graph of the effective diffusion coefficient of H_2O as a function of pore size. The sloping part of the curve represents Knudsen diffusion, while the horizontal branch on the right side of the graph depicts the region of bulk molecular diffusion (figure from Clifford and Hillel 1983, Fig 3).

be possible if the effective pore size of the regolith is much greater than 10 μm, or if the regolith has a specific surface area $\geq 10^3$ m^2 g^{-1}, which would give rise to a diffusive surface flux greater than any likely pore gas flux (Clifford and Hillel 1983). The general picture expected, then, is that ground ice will be found fairly close to the surface at high latitudes, but only hundreds of meters beneath the surface near the equator.

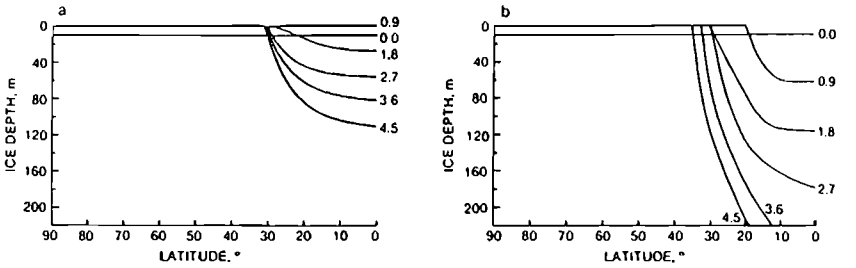

Fig. 5. The depth of ground ice on Mars as a function of latitude and time (Gyr). The regolith models adopted for these calculations differed only in assumed pore size: (a) 1 μm; (b) 10 μm (figure from Fanale et al. 1986, Fig. 5).

D. Groundwater

As discussed by Carr (1979,1986), Baker (1982) and Squyres (1984), the Martian outflow channels provide persuasive evidence that a large reservoir of groundwater was stored in the Martian crust throughout its first Gyr of geologic history (chapter 15). Much of this water may now be stored as

ice in the cryolithosphere. However, once the pore volume of the cryolithosphere has been saturated with ice, any additional subsurface H_2O will inevitably be stored as groundwater.

Under the influence of gravity, groundwater will drain to saturate the lowest porous regions of the crust. Therefore, if we assume that Mars is uniform with a porosity profile everywhere as described by Eq. (1), we can readily calculate the saturated thickness of an aquifer that results from any given volume of water. For example, a quantity of water equivalent to a global layer 10-m deep is sufficient to saturate the lowermost 0.85 km of the porosity profiles seen in Fig. 2; while a quantity of water equivalent to a 100-m layer would create a global aquifer nearly 4.3-km deep (Clifford 1984,1987*b*). However, Mars is not uniform; therefore, the actual self-compaction depth of the megaregolith is expected to have a high degree of variability, restricting the areal coverage of any groundwater system to something $< 100\%$. This restriction in turn means that, for a given quantity of water, the resulting aquifer thickness will locally be greater than that calculated on the basis of global coverage.

If the present inventory of H_2O on Mars exceeds the quantity required to saturate the pore volume of the cryolithosphere, then a subpermafrost groundwater system of substantial proportions could result. This condition may be satisfied by a planetary inventory of H_2O as small as 100 m; however, in no event does it appear that it would require more than 1000 m (Clifford 1984,1987*b*).

E. Permeability

On Earth, the effective permeability of crustal rocks is critically dependent on the scale of the sample under consideration. For example, laboratory measurements of samples several cm in size generally indicate only the minimum permeability of a rock mass (Brace 1980). However, at the scale of interest for most hydrogeologic studies (generally 10^2 to 10^3 m), virtually all crustal rocks have undergone a considerable degree of fracturing, dramatically increasing their effective permeabilities (Streltsova 1976; Legrand 1979; Seeburger and Zoback 1982; Brace 1980,1984).

Despite the relatively low porosity of fractured rock, its permeability can often be quite high (Legrand 1979; Brace 1980; Fetter 1980). This is because the pore geometry of a fracture is inherently more efficient at conducting a fluid, per unit porosity, than the geometry of an intergranular pore network. A rock with a fracture porosity of only 0.011% can have the same permeability as a silt with a porosity of 50% (Snow 1968). The pervasive nature of crustal fractures means that few, if any, geologic materials can be considered impermeable (de Marsily et al. 1977; Fetter 1980; Brace 1980,1984). Brace (1980,1984) has summarized the results of *in situ* borehole permeability measurements and permeabilities inferred from large-scale geologic phenomena (such as earthquakes triggered by fluid injection from

nearby wells) and concludes that on a size scale of ~ 1 km, the average permeability of the top 10 km of the Earth's crust is roughly 10 millidarcies (where 1 darcy is defined as the permeability that will permit a specific discharge of 1 $cm.s^{-1}$ for a fluid with a viscosity of 1 centipoise under a hydraulic pressure gradient of 1 bar cm^{-1}; 1 darcy = 9.87×10^{-13} m^2).

Estimates of the permeability of the Martian crust have generally been much higher. Based on the assumption that each of the Martian outflow channels was carved by a single catastrophic outbreak of groundwater, Carr (1979) calculated the required volume of discharge and necessary permeability of the crust. His calculations suggest that permeabilities as high as 10^2 to 10^3 darcies would be necessary over distances of ~ 10^3 km and to depths of 1 to 2 km. He concluded that permeabilities this high were only reasonable if the Martian crust was intensely fractured and/or possessed numerous unobstructed lava tubes, characteristics similar to those of certain Hawaiian basalts (Davis 1969). However, Carr (1979) also noted that the required discharge and crustal permeability could be reduced 1 to 2 orders of magnitude if the observed relief of the channels was created by shallower flows acting over a longer period of time, or by multiple episodes of groundwater outbreak and erosion.

F. Rheology

As we discuss below, there is morphologic evidence that the Martian regolith in some areas has undergone viscous creep induced by deformation of interstitial ice. Three factors have been found to influence strongly the strain rate of frozen ground undergoing steady-state creep: stress, temperature and regolith structure. The stress dependence of the rheology of ice depends on the deformation mechanism operating at the atomic scale. Two fundamental deformation mechanisms are possible: diffusion of atoms and movement of dislocations in the crystal lattice. For diffusion creep, the strain rate is roughly proportional to the applied stress; i.e., the material has a Newtonian rheology. For dislocation creep, the strain rate is proportional to stress to some power n, where n is typically ~ 3. Whether diffusion or dislocation creep dominates in ice depends on stress, on temperature and on grain size (Shoji and Higashi 1978). Both mechanisms could operate in the Martian regolith during the deformation of a given topographic feature, perhaps at different times and at different depths.

The temperature dependence of ice and frozen soil rheology is relatively well understood. The rate of steady-state creep is generally proportional to $\exp(-Q/kT)$, where T is temperature, k is Boltzmann's constant and Q is the activation energy of the deformation mechanism. This temperature dependence should have a significant influence on regolith rheology as a function of latitude, with mobility substantially inhibited at latitudes higher than 50 to 60° (Lucchitta 1984*a*; Squyres and Carr 1986; Squyres 1989*c*).

The most important determinant of the rheology of an ice-silicate mix-

ture can be the structure of the mix; that is, the relative proportions of ice and silicate and the way in which the grains interact. Depending on structure, the material can be as mobile as pure ice, or as rigid as pure rock. At small silicate concentrations in an ice-silicate mixture, grains of rock act as particles in suspension in the ice. They do not deform appreciably in response to stress, and a comparatively higher strain rate in the ice is required to provide a given bulk deformation rate for the mix as a whole. When the volume fraction of silicates exceeds about 0.5 to 0.6, however, the physical manner in which the grains and ice come into contact (the regolith "structure") becomes crucially important in controlling the rheology of the mix. If the silicate material is thoroughly comminuted and disaggregated, forming a true soil, then significant mobility still is possible at very high silicate fractions (see, e.g., Andersland and Akili 1967; Ersoy and Togrol 1978; Haynes 1978). However, other possible structures can have substantial ice content, but have rheologic properties controlled by the rheology of the rocky component. Fractured bedrock, in which large fractures have been produced but complete disaggregation, comminution and re-orientation of blocks have not taken place, can have such characteristics. As the transition is made from comminuted soil near the surface to solid bedrock below, structural effects will cause mobility of the Martian regolith to decrease with depth, dropping it to zero at some depth where the rheology becomes controlled by rock rather than ice.

II. POTENTIAL MORPHOLOGIC INDICATORS OF GROUND ICE

Many physical properties of the Martian regolith can be expected to have an impact on the present distribution of ice beneath the surface. Based on expected regolith properties and estimates of the total Martian H_2O inventory, one may infer a likely distribution of ground ice like the one shown in Fig. 5. However, the distribution may also be inferred directly from observation of morphologic features on the planet's surface. In the sections that follow, we discuss several Martian geomorphic features that may provide evidence for the former or present existence of ground ice. We also describe the geographic distributions of the major features, and compare them to the predictions of thermodynamic models.

A. Rampart Craters

1. Morphology. Most large craters on Mars for which distinct ejecta blankets can be observed have ejecta morphologies that are very different from those observed on, for example, the Moon. Large Martian craters typically have an ejecta sheet with a pronounced low ridge or escarpment at its outer edge. The ejecta sheet commonly has a distinctly lobate outer margin, giving the appearance of a flow formed by the rapid outward spread of a

highly mobile fluid. Larger craters may have several overlapping sets of flow lobes. The flows can bury a variety of topographic features in the underlying terrain, and appear massive enough to contain the majority of the total ejecta from the crater. Craters possessing such ejecta are referred to as rampart craters (chapter 12). The morphology of rampart craters strongly suggests that ejecta were emplaced primarily as radially directed surface flow, rather than ballistically. The most convincing evidence for fluid emplacement is the geometry of the flow lobes, and particularly the observation that they can be diverted around relatively small pre-existing topographic obstacles, rather than draped over them (Carr et al. 1977*b*).

The most likely explanation for the morphology of rampart craters is that their ejecta were emplaced as a mud flow. The water entrained in the ejecta apparently was derived from beneath the Martian surface. In fact, a number of the basic morphologic characteristics of the craters can be duplicated by high-velocity experimental impacts into mud (Gault and Greeley 1978). Significant questions still concern the role of the atmosphere in the development of fluidized ejecta deposits, and it has been suggested that certain aspects of rampart crater morphology are due to atmospheric effects rather than to the presence of subsurface H_2O (Schultz and Gault 1979; Schultz 1986). It also is not clear whether the subsurface H_2O that may have been involved was in the liquid or solid state at the time of the impact (See the discussion of lobate ejecta craters in chapter 12.) For the purposes of our discussion here, however, we will accept what we believe to be the most probable explanation for rampart craters, namely that they result from melting of subsurface ice during the impact process.

2. *Distribution.* Rampart craters with a wide range in diameters constitute a considerable fraction of all the craters on Mars. As has been found by many investigators (Carr et al. 1977*b;* Allen 1978; Mouginis-Mark 1979; Kuzmin 1980*a*,1983; Horner and Barlow 1988; Costard 1989), rampart craters are present in almost every major geologic unit on Mars and at all latitudes from the equator to the edges of the polar caps. They have formed at altitudes ranging from nearly the lowest on Mars to over 8 km above the planetary datum. Despite their ubiquitous nature, however, they show important regional and global trends in their morphology and morphometry that may be used to make a number of inferences about the subsurface distribution of H_2O on Mars.

From the physics of the impact process (Croft et al. 1979; Croft 1984; Kieffer and Ahrens 1980; Chapman and McKinnon 1986; Melosh 1989) it is known that vaporization and melting of ground ice at the moment of impact may occur in the part of the subsurface that is shocked to roughly 10 to 100 GPa. The volume of such a zone is directly related to the crater's size; it becomes larger with an increase in the crater's diameter (Ivanov 1986). If the origin of the fluidized ejecta is connected with the vaporization and the melt-

ing of ground ice, then fluidized ejecta may be produced in cases where crater excavation depths are greater than the depth to the top of an ice-rich layer in the regolith.

A fundamental observation concerning rampart craters is that, in a given area, a certain critical crater size exists (Boyce 1980; Kuzmin 1980*a*); craters smaller than this size lack fluidized ejecta, while craters larger have it. This crater size, called the onset diameter, is in some sense an indicator of the depth to which an impact event must excavate to reach significant quantities of ice. Mapping of onset diameters as a function of geographic location on Mars therefore may allow a good semi-quantitative test of the ground ice distributions predicted by the thermodynamic models discussed above.

The most complete statistical studies of the geographic distribution of rampart craters have been performed recently by Costard (1988,1989) and Kuzmin et al. (1988*b*,1989). These studies involved characterizing the morphology, morphometry and location of over 10,000 Martian rampart craters. Figure 6 shows the geographic distribution of onset diameters. The most important finding is that there is a pronounced dependence of onset diameter on latitude. Near the equator, onset diameters are typically 4 to 7 km. At latitudes of 50 to 60°, however, they decrease to just 1 to 2 km. Apparently, the depth to ground ice (i.e., the thickness of the desiccated upper layer of the regolith) is substantially greater near the equator than it is at high latitudes. This result is in agreement with predictions of thermodynamic models: loss of ground ice has proceeded to the greatest depths at the lowest latitudes.

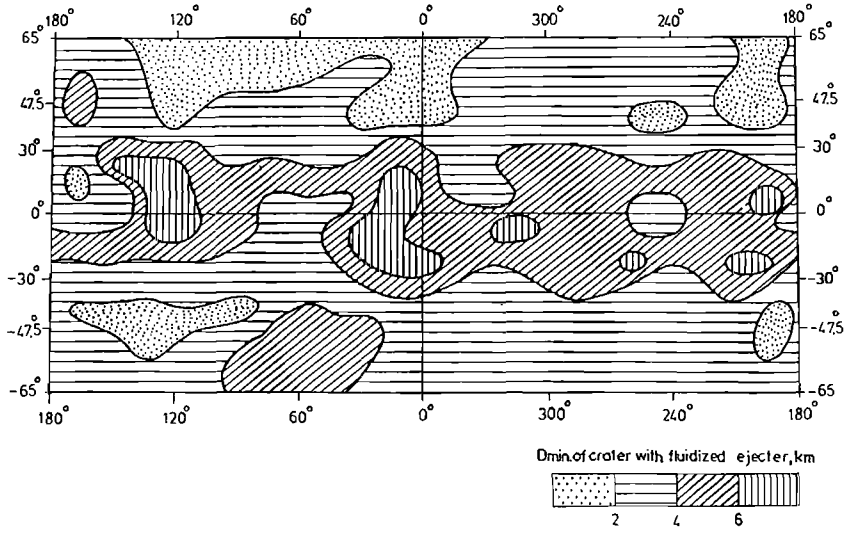

Fig. 6. The geographic distribution of rampart crater onset diameters on Mars. Onset diameters are greatest near the equator, indicating that the depth to ground ice is greatest in this region.

Interpreting the geographic distribution of onset diameters in terms of an absolute depth to the top of an ice-rich layer is a somewhat more difficult problem. The issue is complicated by several factors. First, it is not immediately clear how deeply the impact must excavate into the ice-rich layer for an observable fluidized ejecta deposit to develop. The answer probably depends on the concentration of ice in the lower layer; deeper penetration of this layer will be required for lower ice content. A second problem is that thermodynamic considerations suggest that the thickness of the upper desiccated zone should increase gradually over time. Since the craters in a given area may have formed over some significant time interval, they may sample a range of ice depths, blurring the quantitative conclusions reached from onset diameters. Nevertheless, attempting to infer ice depth from onset diameter is instructive, and this approach has been taken by Kuzmin et al. (1988*b*, 1989). For this work, a relationship between observed crater diameter and the depth of the crater's transient cavity was used, derived from the physics of the impact process (Stoffler et al. 1975; Croft 1980,1984; Ivanov 1988*a*). It was assumed that any penetration of the ice-rich layer by the transient cavity would be sufficient for fluidized ejecta formation. This assumption should yield an upper limit on the depth to the ice-rich layer at the time of impact. A map of the depth to ground ice on Mars derived in this manner is shown in Fig. 7. Under the assumptions made, the thickness of the desiccated upper

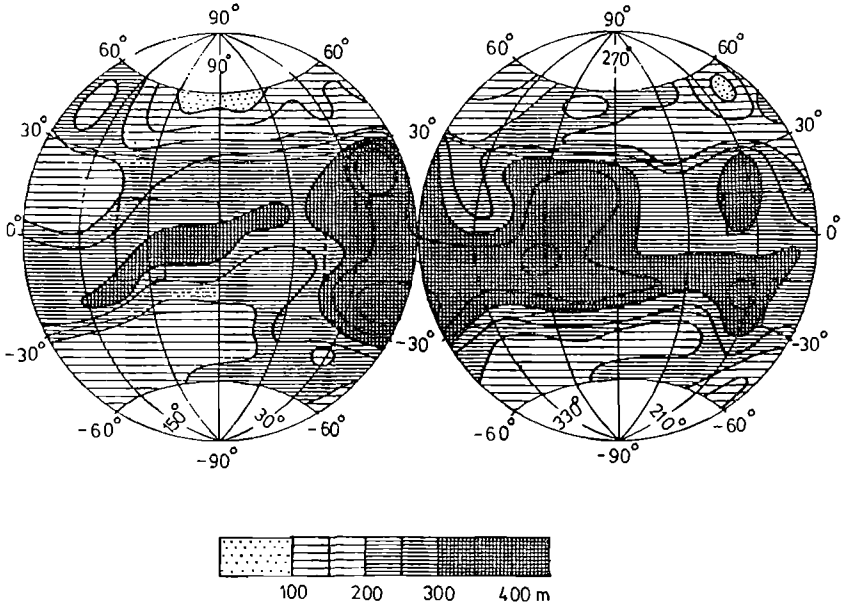

Fig. 7. Depths to the top of an ice-rich zone in the Martian regolith derived from the map in Fig. 6 and assumptions about the nature of the rampart crater formation process.

zone of the regolith is typically 300 to 400 m near the equator. At 30° latitude the roof of the ice-rich zone rises to 200 to 250 m, and at 50° latitude to 100 m. As a rule, the maximum roof depths in equatorial regions are localized in the more elevated areas of the planet (e.g., Syria Planum, Noctis Labyrinthus, Elysium Planum) or in the oldest and highest areas of the cratered terrain within the southern highlands. Roof depths are slightly greater in the southern hemisphere than in the northern hemisphere.

It is difficult to determine quantitatively the ice content of the subsurface materials. An assessment of the relative ice content may be possible, however. The basic technique that has been applied to this problem is measurement of the ratio of the fluidized ejecta blanket diameter to the crater diameter (Kuzmin et al. 1988*b*; Costard 1988). The assumption made is that relatively more extensive fluidized ejecta deposits indicate a higher concentration of ice in the ice-rich subsurface layer. Figure 8 shows the variation of this ratio as a function of latitude for two different ranges of crater diameter. These data suggest that the concentration of ice in the ice-rich subsurface materials increases with increasing latitude. They also suggest that the regolith of the northern hemisphere is somewhat more ice-rich than that of the southern hemisphere. The reason for this asymmetry may be that the northern plains of Mars were the primary areas of accumulation for the great Martian outflow channels. As the water from these floods pooled and soaked into the ground, it could have substantially enriched the ice content of the underlying regolith.

In summary, study of rampart craters and mapping of their morphologic

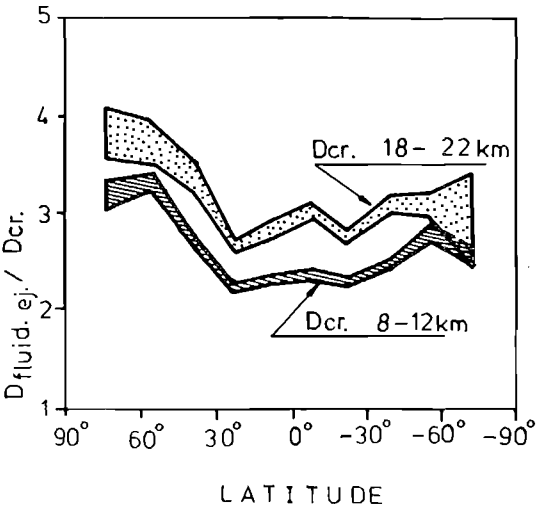

Fig. 8. Ratio of fluidized ejecta sheet radius to crater radius, as a function of latitude, for two size ranges of Martian craters. The ratio increases with latitude, suggesting that subsurface regions may be relatively richer in ice at higher latitudes.

and morphometric parameters shows that the main feature of the Martian cryolithosphere is a latitudinal zonality, with prominent desiccation of shallow layers at the equator. This inferred distribution of ice is in excellent qualitative agreement with the predictions of thermodynamic models. The ice concentration appears greater and the spatial distribution somewhat more complex in the northern hemisphere than the southern one, perhaps reflecting the processes that have been responsible for emplacement of the ground ice in the north.

B. Debris Flows and Terrain Softening

Another important way in which subsurface ice can influence the morphology of a planetary surface is by promoting slow creep and flow in the solid state. By geologic standards, ice is an extremely mobile material. Ice-rich permafrost on Earth can undergo substantial deformation as the ice that cements the soil deforms and flows in the solid state (Thompson and Sayles 1972; Phukan 1983; Sadovsky and Bondarenko 1983; Weerdenburg and Morgenstern 1983). Rock glaciers, which are found in many arctic and alpine environments, are rock-ice masses that deform and flow due to solid-state creep in the ice that cements the rocky debris; again, no thawing is involved (Ives 1940; Wahrhaftig and Cox 1959; Thompson 1962; White 1976). We discuss here two classes of Martian landforms that result or may result from viscous creep of near-surface materials. The first class is formed of materials that have been loosened from their original locations, transported down an escarpment by mass-wasting, accumulated at the base of the escarpment, and undergone subsequent creeping flow. These debris flows include *lobate debris aprons, lineated valley fill,* and *concentric crater fill* (Squyres 1978,1979*a*). They may be directly analogous to terrestrial rock glaciers. The second class, called *terrain softening,* is really a style of landform degradation produced by viscous deformation of material *in situ.* It is more directly analogous to the solid-state deformation observed in terrestrial permafrost, or to the relaxation of topography that is observed on some icy satellites in the outer solar system.

1. Debris Flows. Lobate debris aprons (Fig. 9) are thick accumulations of debris at the bases of escarpments. Their most noteworthy morphologic characteristic is their pronounced convex topography. The surface of the debris apron slopes gently away from the source escarpment, and then steepens to form a distinct flow terminus. This morphology is a clear indication that deformation and flow have taken place throughout a substantial thickness of the deposits. Lobate debris aprons can exhibit distinctive surface lineations (Squyres 1978), both parallel and transverse to the flow, that have counterparts in terrestrial rock glaciers (Wahrhaftig and Cox 1959).

Lobate debris aprons are very common in some areas, particularly in the fretted terrain separating the northern lowlands from the southern highlands between 280 and 350° longitude. In locations where flows commonly run up

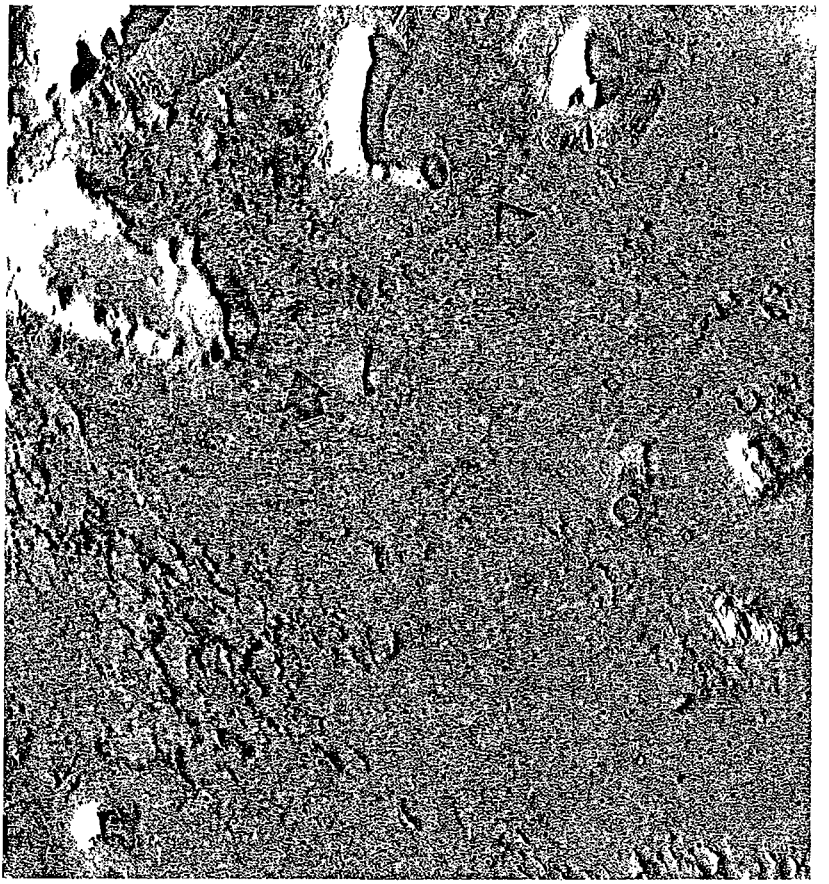

Fig. 9. Lobate debris aprons (arrows), showing the convex topographic profiles commonly exhibited by these features. (Viking Orbiter image 58B51; latitude 47°, longitude 325°. Image width is ~ 90 km.)

against opposing escarpments or against one another, complex patterns of flow and compressional lineations can form. An extreme case is shown in Fig. 10. Here the debris has been confined entirely in narrow valleys. The pervasive obstruction of flow outward from the valley walls has produced many compressional lineations parallel to those walls. These valley-floor deposits have been termed lineated valley fill (Squyres 1978). They are composed of the same material that forms the lobate debris aprons, and are the other end-member of a continuum of landforms produced by this material in the fretted terrain.

Another class of landforms that has been interpreted to be formed from flow of ice-cemented erosional debris is shown in Fig. 11. Material is ob-

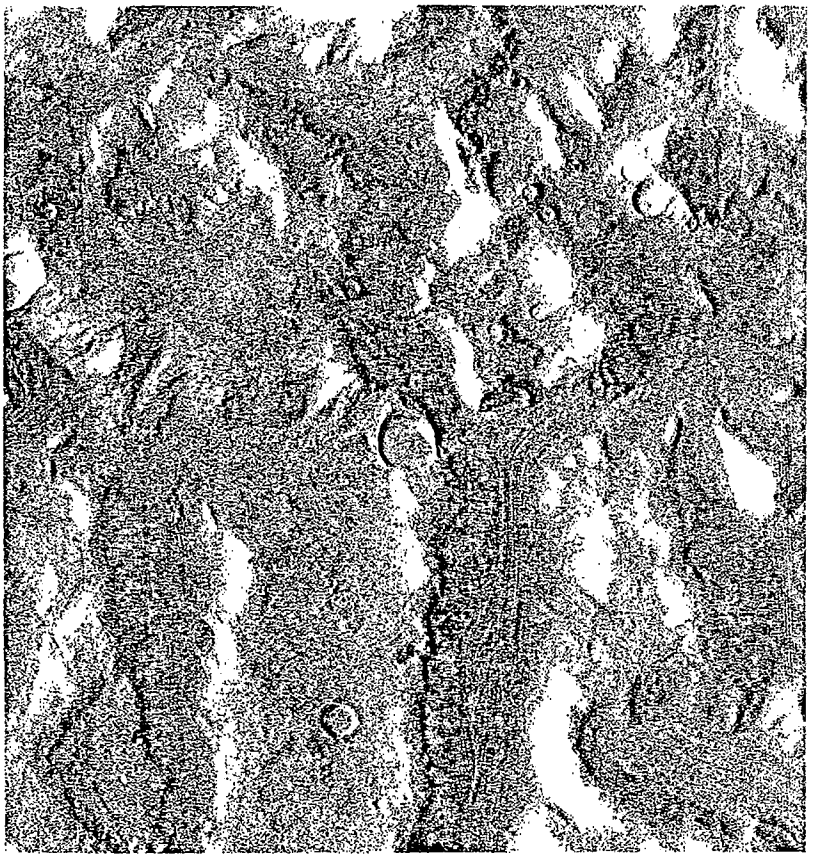

Fig. 10. Lineated valley fill, apparently composed of the same kind of material that makes up lobate debris aprons. (Viking Orbiter image 84A73; latitude 34°, longitude 290°.)

served on the floors of craters with a distinct, crudely concentric pattern of ridges and troughs. Such deposits have been called concentric crater fill (Squyres 1979*a*), and the topography has been interpreted as resulting from compressional stresses generated by inward flow of ice-rich material from the crater walls.

The interpretation of most concentric crater fill as having resulted from ice-aided flow is less clear cut than is the case for lobate debris aprons and lineated valley fill. Arguments in support of this view include the morphologic similarity between concentric crater fill and the other types of flows, the observation of landforms transitional between lobate debris aprons and concentric crater fill (Squyres 1989*c*), and the fact that the geographic distributions of all three types of features are similar and consistent with theoretical predictions of ground-ice stability (see below). An alternative view of con-

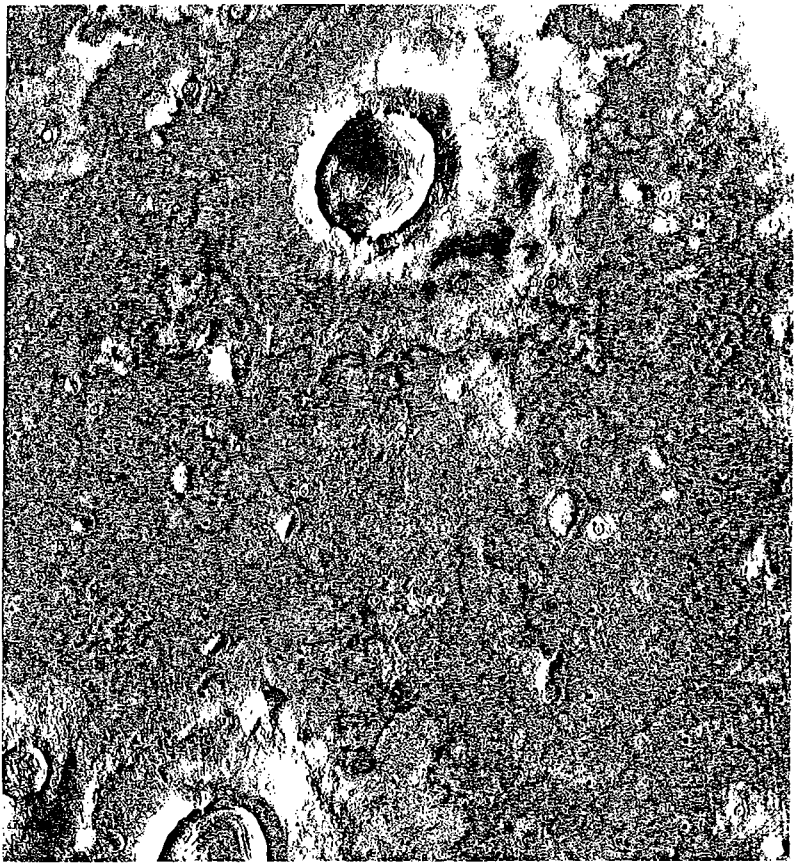

Fig. 11. Impact craters in Utopia Planitia containing concentric crater fill. (Viking Orbiter image 10B70; latitude 42°, longitude 272°.)

centric crater fill, however, is that much of the observed morphology is aeolian in origin. High-resolution (< 10 m/pixel) images of materials both within and surrounding craters in the Utopia region (45°N, 271°W) show an eroded, multiple-layer deposit emplaced on the cratered topography, most likely by aeolian processes (Zimbelman et al. 1989). Such layering would not be preserved well if the material moved by slow deformation throughout its thickness. It is likely that both ice-related and aeolian processes have been active throughout the Martian midlatitudes, so that care must be exercised in attributing concentric crater fill morphology to ground ice in areas where high-resolution images are lacking.

2. Terrain Softening. Terrain softening is a distinctive style of landform degradation observed in some regions on Mars. It affects landforms of

all types, but one type of landform on which it is particularly evident is impact craters. An example is given in Fig. 12. The first image (a) of the pair shows craters in normal, i.e., unsoftened, terrain. The second image (b) presents a similar scene in softened terrain. The differences are striking. In the unsoftened terrain, the topography is crisp and rugged. Crater rims are sharp. Crater walls are blocky and angular, with slope profiles that are dominantly straight or concave upward. Between large craters are low but angular ridges and hills. In the softened terrain, however, crater rims are broad and gently rounded. Crater walls preserve their blocky nature to some degree, but the individual blocks are softly rounded rather than angular. Slope profiles of crater walls are dominantly convex upward. The terrain between large craters has a smooth rolling character and lacks the angular ridges and hills characteristic of unsoftened terrain. Terrain softening is by no means limited to impact craters, and affects all manner of topographic features (Squyres 1989*c*). In all cases, the effects are the same: terrain softening produces broad rather than sharp slope inflections, and convex rather than concave slope segments.

Before attributing terrain softening to ice-induced creep, however, alternative causes for the observations must be considered. Processes that might contribute include atmospheric obscuration and burial by aeolian debris. Suspended aerosols can degrade the detail visible in Viking images at high spatial frequencies, and periods of high opacity should be avoided in statistical studies (Kahn et al. 1986). However, examination of images of unsoftened terrain acquired during times of even very high atmospheric opacity still clearly show the crisp nature of the topography (Squyres 1989*c*). Aeolian mantling may contribute significantly to a general muting of topography, and clearly has taken place in some areas on the planet. Soderblom et al. (1973*b*) concluded on the basis of Mariner 9 images that the middle-to-high latitudes of Mars are largely blanketed with aeolian debris, and layered deposits observed within and around some impact craters appear to confirm that widespread, perhaps cyclic mantling has taken place in some midlatitude regions. High-resolution Viking images show that both creep and mantling processes have operated on Mars, with creep being most important at the middle latitudes and mantling most important at higher latitudes. Discriminators between the effects of mantling and creep include (a) the observation that aeolian debris tends not to accumulate readily on sharp, exposed ridge crests, so that such features commonly remain sharp even in mantled terrains; and (b) the tendency of mantling to most effectively remove the smallest topographic features, while creep preserves small features as the stresses they generate are insufficient to lead to their relaxation. Because of the importance of aeolian blankets on Mars, these discriminators must be applied with care when inferring the distribution of subsurface ice on Mars from terrain softening.

Color Plate 9 presents a map of the distribution of viscous creep features on Mars (Squyres and Carr 1986), compiled with consideration of the key

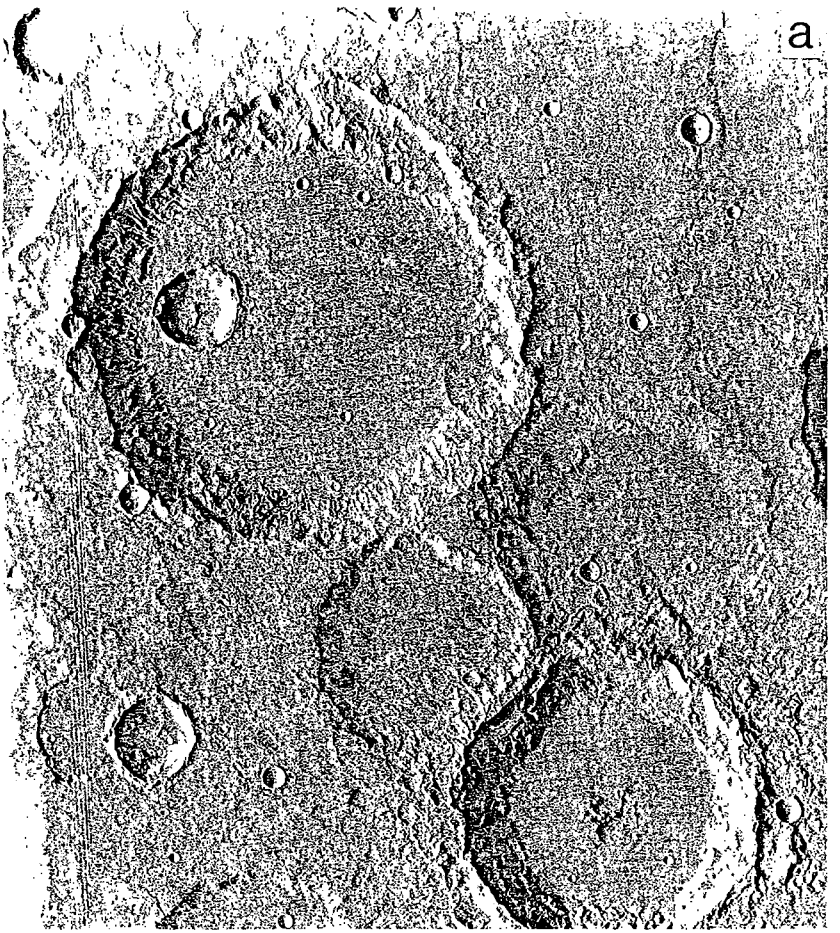

Fig. 12. Images showing unsoftened (a) and softened (b) terrain. (Viking Orbiter image 423S10; latitude − 32°, longitude 227° with image width ~ 160 km. Viking Orbiter image 195S20; latitude 33°, longitude 313° with image width ~ 60 km.)

morphologic discriminators for creep deformation. The features observed are grouped into three classes: (1) lobate debris aprons and lineated valley fill; (2) concentric crater fill; and (3) creep-related terrain softening. The distribution shows a pronounced variation with latitude. Virtually no creep features are found within 30° of the equator. In the northern hemisphere, lobate debris aprons and lineated valley fill are most common in Tempe Fossae, Mareotis Fossae, the Phlegra Montes, in a small region of old cratered terrain north of Olympus Mons, and particularly in regions of fretted terrain. Concentric crater fill is found in most of these areas, and also is common on Utopia Planitia. In the southern hemisphere, lobate debris aprons/lineated valley fill and con-

centric crater fill are most common in regions adjacent to the Hellas and Argyre basins. Creep-related terrain softening in the northern hemisphere is present in all areas where the ancient cratered highlands extend north of 30° latitude. Cratered highlands dominate the southern hemisphere, and most regions observed south of −30° latitude exhibit some degree of creep-related terrain softening. It is ubiquitous in the midlatitudes, and becomes less pronounced toward the south pole. The distribution of creep features in Plate 9 again is broadly consistent with thermodynamic predictions of ground-ice stability. Where the calculations indicate that ground ice should be stable close to the Martian surface, creep features are observed in abundance. Where they indicate that ice is unstable near the surface, creep features are essentially absent.

There is also a change in the style and prevalence of creep-related terrain softening over the latitudes where it is observed. At middle latitudes (30 to ~ 55°), it is common and has the morphologic characteristics already described. At higher latitudes, however, it becomes much less widespread and pronounced, and other creep features (lobate debris aprons, etc.) disappear altogether. Crater rims are sharper than at the middle latitudes, and intercrater areas are rougher. The decrease in the observed frequency and extent of creep-related terrain softening at high latitudes is most likely due to the colder temperatures and higher viscosities found there.

Images of softened terrain convey the impression that the creep that apparently produces it is a relatively near-surface phenomenon. This impression can be investigated with a simple finite-element model of crater relaxation in a viscous medium overlying a rigid substrate (Squyres 1989*c*). Results are shown in Fig. 13. At the top of the figure is the profile of a fresh 20-km crater before deformation. The lower part shows the crater after roughly equivalent amounts of relaxation for 4 thicknesses of the deforming layer: 20, 5, 2.5 and 2 km. With relaxation in a deep viscous layer, the longest topographic wavelengths are removed most rapidly, producing a pronounced upwarping of the crater floor and leaving the crater rims sharp. As the depth to the rigid substrate becomes smaller, however, deep rim-to-bowl flow is suppressed, and the crater floor remains flat. The rim is lowered, and is broadened significantly. The profile of the crater walls is altered markedly, from concave to distinctly convex. This is the style of deformation observed in creep-related terrain softening. These results indicate that the thickness of the deforming

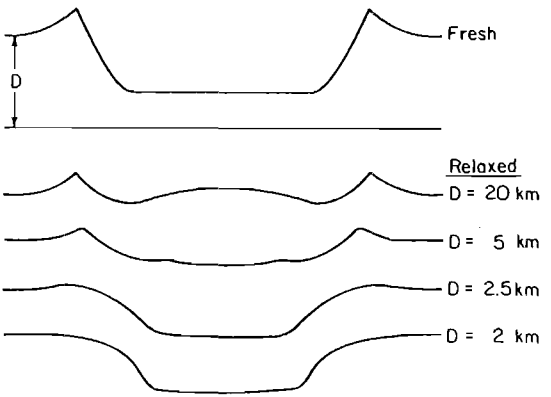

Fig. 13. Results of finite-element calculations of relaxation of a crater in a viscous material overlying a rigid substrate. Upper profile shows the topography of the initial crater, with a vertical exaggeration of 2.5 times. Lower 4 profiles show topography at the same vertical exaggeration after comparable amounts of relaxation for 4 different thicknesses of the viscous layer. In order to produce topography like that observed in softened terrain, the viscous layer thickness must be a small fraction of the crater diameter.

layer must be a very small fraction of the diameter of the relaxed crater to produce the observed morphology by viscous relaxation.

C. Other Possible Morphologic Indicators of Ground Ice

Several other morphologic features on Mars have been proposed as potential indicators of the presence of H_2O within the near-surface materials. Many such features involve the former presence of zones within the cryolithosphere (taliks) where temperatures were above the freezing point, and liquid water could have been present. These features are thoroughly reviewed elsewhere (see e.g., Carr and Schaber 1977; Rossbacher and Judson 1981; Lucchitta 1985*a*) and only some of the more widely cited landforms are discussed here. Along with a description of each feature, we include a brief discussion of the primary arguments for and against a direct association with subsurface volatiles.

1. Chaotic Terrain. This landform consists of lowland areas separated from cratered uplands by abrupt escarpments and displaying a rough floor topography with a haphazard jumble of large angular blocks and arc-shaped slump blocks (Sharp 1973*a*). The interpreted formation process involves collapse induced by removal of subsurface water or ice (Carr and Schaber 1977). Evidence in support of an origin related to ground ice includes several examples of large outflow channels that extend downslope from areas of chaotic terrain, indicating a probable causal relationship between the eroding fluid and the chaotic terrain. Sharp (1973*a*) reviews several possible hypotheses for the formation of chaotic terrain, including withdrawal of either subsurface ice or magma and the flow of groundwater, and concludes that all three mechanisms could have been involved. Carr (1979) supports the dominant role of groundwater by suggesting that release of water from a confined aquifer could explain the common association between chaotic terrain and outflow channels.

2. Thermokarst. This is the process whereby melting of ground ice causes local collapse and formation of rimless depressions (alases) which generally are roughly circular in outline and flat floored (Carr and Schaber 1977). Features interpreted to be possible alases have been observed in Chryse Planitia and near Maja Vallis (Theilig and Greeley 1979) and Ares Vallis (Costard 1987). An example is shown in Fig. 14. Along the irregular outline of the cliff which may have resulted from coalescing alases is a band of higher albedo that may relate to a change in the tableland materials in proximity to the cliff (Carr and Schaber 1977). Discrete ice lenses within the Martian surface material could enhance the efficiency of thermokarst development (Lucchitta 1985*a;* Costard and Dollfus 1987). The presence of isolated, buried ice deposits at equatorial latitudes is consistent with the interpretation of entrained ice in some fluidized landslides within Valles Marineris

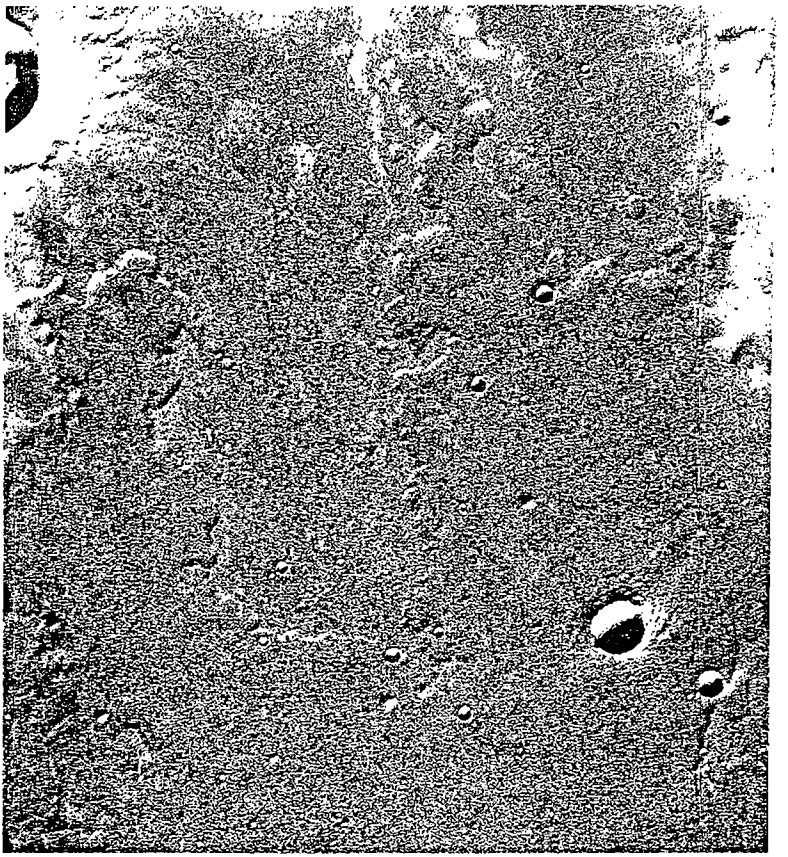

Fig. 14. Possible thermokarst terrain in the southern part of Chryse Planitia, as identified by Carr and Schaber (1977). Small depressions in the plateau area appear to enlarge and merge as the plateau is destroyed, quite possibly through the removal of ground ice with subsequent slope failure. An albedo feature that follows the outline of the cliff may indicate some change in the plateau materials caused by proximity to the cliff. (Viking Orbiter image 8A70, latitude 23°, longitude 36°. Image width is ~ 50 km.)

(Lucchitta and Ferguson 1983; Lucchitta 1987*c*), although these features are not associated with a thermokarst source. Devolatilization from ice lenses exposed by channel formation may contribute to the cuspate banks observed along some Martian channels, analogous to thermocirques present in Siberia (Czudek and Demek 1970).

Arguments in favor of the features cited above being thermokarst are numerous well-documented cases of terrestrial features similar in size and morphology that occur in regions possessing 80 to 90% (by volume) of ground ice (Washburn 1973; Soloviev 1973). The main argument against a ground-ice origin is the possibility of alternative methods for eroding the

tablelands without the required presence of a subsurface volatile, such as dry mass wasting in a vertical section possessing variable competency.

3. Patterned Ground. This category consists of a variety of features including circles, polygons, nets and stripes, all of which are associated on Earth with ice wedging in periglacial regions (Washburn 1973). Polygons are the dominant form of patterned ground identified on Mars. The polygons on Mars found in close proximity to polar ice deposits (Fig. 15a) typically are at least an order of magnitude larger than comparable ice-related features on Earth (Rossbacher and Judson 1981). The troughs defining them have upturned edges similar to cracks associated with active terrestrial ice-wedge polygons (Lucchitta 1981).

Mechanical considerations make it unlikely that the giant polygons, with diameters of up to 20 km, are the result of thermal cracking (Pechmann 1980). Strong arguments have been presented that the giant polygons in the northern plains of Mars may be due to fracturing of a layer of sediment deposited over ancient heavily cratered terrain, a scenario not requiring the presence of ice wedges (McGill 1986). This scenario is consistent with other features in the northern lowlands that are interpreted to be sediments derived from the southern highlands, transported through the numerous outflow channels that debouch on the northern lowland plains (Lucchitta et al. 1986).

Polygons in the size range consistent with terrestrial periglacial polygons also have been identified in high-resolution images of Mars (Fig. 15b; Evans and Rossbacher 1980; Lucchitta 1983). These small features cover a much more restricted region than the more prominent large polygons. They have good potential for being related to periglacial processes, but the origin of the giant polygons is ambiguous.

4. Pseudocraters. These landforms are closely spaced cinder cones, generally < 100 m across, derived from phreatic eruptions where lavas have been emplaced over materials containing either abundant groundwater or ice (Thorarinsson 1953). In the Cydonia Mensae region of Mars, numerous small, aligned domes are present, some of which have summit depressions (Frey et al. 1979; Allen 1979). The mounds are near the limit of resolution in most images, so that a phreatic eruption origin cannot be directly verified. Pseudocraters may be useful in providing supporting evidence for the presence of subsurface volatiles, but their uncertain origin makes them an ambiguous indicator by themselves.

5. Pingos. These landforms are domelike mounds with ice-cored interiors that result from the injection of groundwater, perhaps aided by freezing of the surrounding ground (Flint 1971, p. 280). Degraded pingos are characterized by summit craters (Rossbacher and Judson 1981), and the collapse depressions on pingos usually have an irregular shape (Lucchitta 1985).

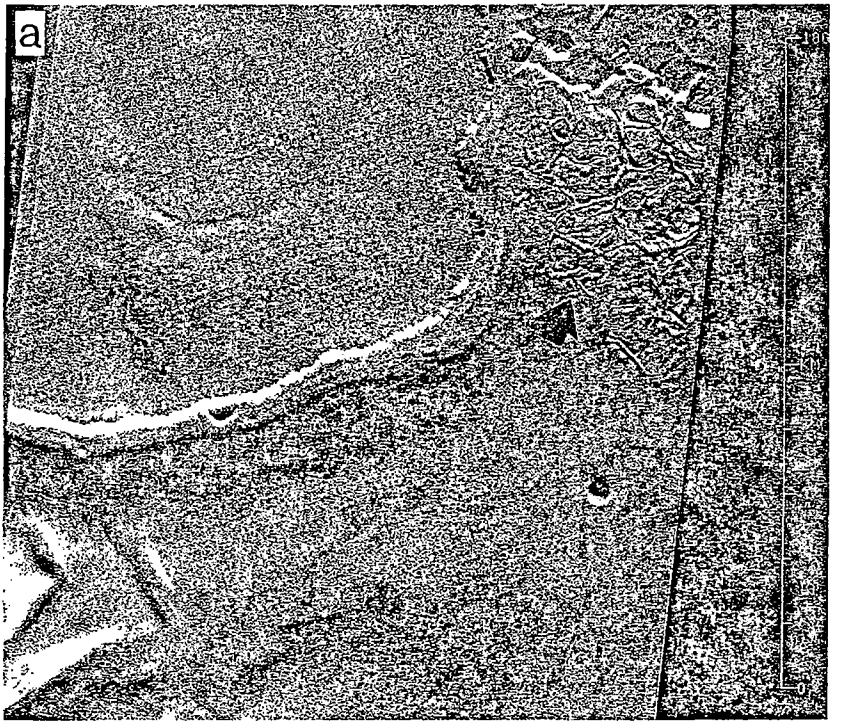

Fig. 15. (a) Polygonally fractured patterned ground near the margin of the north polar ice cap on Mars. Note that the troughs making up the polygons have raised edges, similar to active ice-wedge polygons on Earth (Lucchitta 1981). Individual polygons range from 2 to 10 km in diameter. (Viking Orbiter image 56OB42, latitude 81°, longitude 63°. Image width is ~ 115 km.) (b) Polygonally fractured patterned ground in the Deuteronilus Mensae region of Mars. The polygons range from 50 to 300 m in diameter, much closer in scale to polygonal ground on Earth than the polygons in (a). (Viking orbiter image 458B67; latitude 47°, longitude 346°.)

These characteristics are similar to those of the possible pseudocrater mounds on Mars discussed above, but once again the Viking image resolution is insufficient to provide conclusive evidence for or against an ice-related origin (Rossbacher and Judson 1981; Lucchitta 1981, 1985). Support for the possibility of pingos on Mars comes from the association of a few mounds with alases (Theilig and Greeley 1979), but most Martian mounds with summit craters are considerably larger than the largest pingos on Earth (Coradini and Flamini 1979). Thermodynamic constraints (Coradini and Flamini 1979) make it unlikely that significant quantities of near-surface water would be available for injection into Martian pingos, and indeed suggest that near-surface freeze thaw should not play a significant geomorphic role under the present Martian climate.

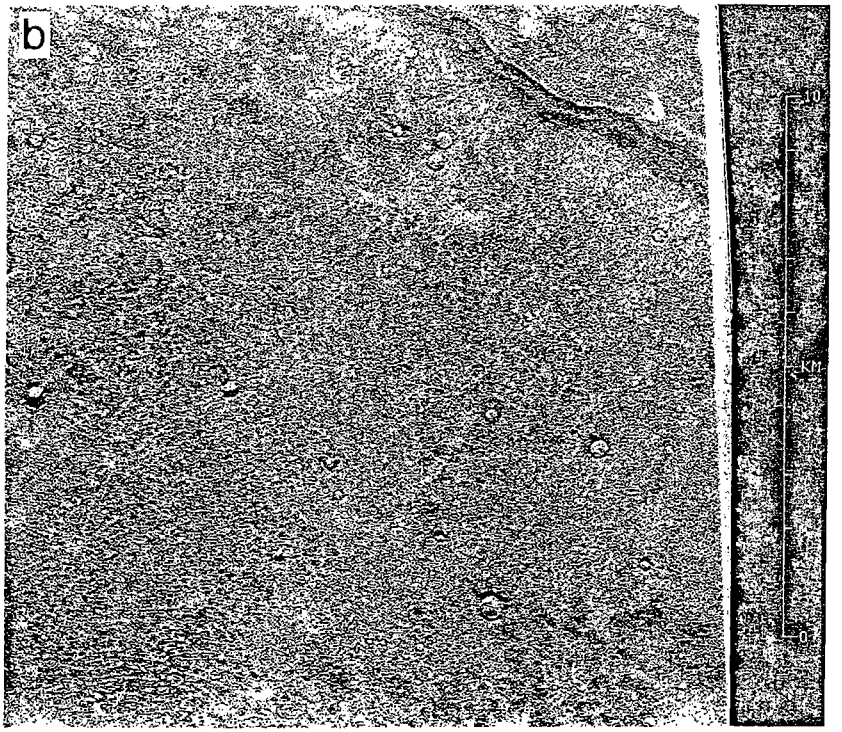

6. Table Mountains. A common landform in Iceland, these form when volcanic eruptions occur beneath a thick cover of ice, producing steep-sided mountains topped by gently sloped volcanic flows (Jones 1970). Features similar to table mountains have been identified in the northern plains of Mars (Hodges and Moore 1979; Allen 1979) but, with the rather extreme exception of Olympus Mons (Hodges and Moore 1979), definite evidence of volcanic materials on top of the Martian mesas is lacking. While a large amount of H_2O may exist on Mars, it is not likely that a great deal of this water was ever on the surface at one time or frozen into km-thick sheets of ice. Without clear evidence of a volcanic center on the Martian mesas, then, these features cannot be considered reliable indicators of the presence of ice.

7. Curvilinear Ridges. Ridges in concentric arcs with lengths of tens of km and spacing of 2 to 5 km are common at certain locations on Mars, particularly in the northern lowland plains. The curvilinear pattern gives a "fingerprint" appearance to the plains (e.g., Fig. 16). The origin of these features is problematic at best (Rossbacher and Judson 1981). There is no direct evidence of involvement of volatiles in the generation of the curvilinear features, but they have been related to erosion of midlatitude mantling mate-

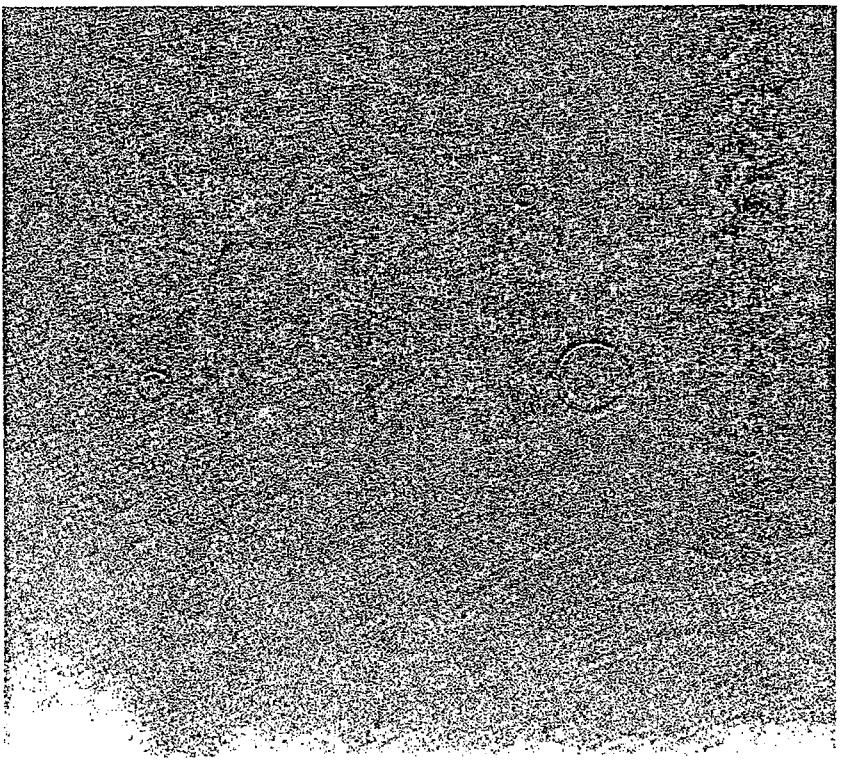

Fig. 16. Curvilinear ridges on the northern plains, arranged in patterns similar to what is observed in some periglacial patterned ground on Earth. (Viking Orbiter image 57B56, latitude 50°, longitude 287°; scale across frame is about 90 km.)

rial (Carr and Schaber 1977), glacial moraines (Lucchitta 1981), and an ancient volatile-rich debris layer in Isidis Planitia (Grizzaffi and Schultz 1989).

Finally, a whole range of other surface features have been related to possible localized reservoirs of subsurface H_2O. Examples include fluidized landslide deposits with associated fluvial channels present within Valles Marineris (Lucchitta 1987*c*), debris aprons next to the northwest flanks of the large shield volcanoes of Tharsis interpreted to result from glacier-like creep of localized ice deposits (Lucchitta 1981), crater chains near Valles Marineris resulting from collapse over a zone of preferential melting of ground ice (Lucchitta 1981), and ridges with bounding depressions, both near the mouths of Martian outflow channels (Lucchitta et al. 1986) and on smooth plains within an impact basin (Grizzaffi and Schultz 1989).

III. DISCUSSION AND SUMMARY

We have discussed above a number of possible morphologic indicators of ground ice on Mars, concentrating on rampart craters and terrain softening. An important observation is that detailed mapping of these two classes of features appears at first glance to lead to different conclusions. Rampart craters are seen at all latitudes, while terrain softening is only observed poleward of ± 30°. In order to form a consistent picture of the distribution of ground ice on Mars, we need to resolve this apparent inconsistency.

As discussed above, the Martian regolith is primarily a product of intensive impact bombardment coupled with volcanic and weathering activity. Near the surface, materials in heavily cratered terrains are dominated by disaggregated and pulverized impact ejecta. This grades downward into bedrock that has been extensively fractured in place and, finally, into solid bedrock below. Because regolith structure can exert a dominant influence on the rheology of ice-rich ground, one would expect such a structure to lead to an abrupt decrease in regolith mobility at some depth, perhaps not more than several hundred m below the surface. If this is the case, then the differences between the distributions of rampart craters and terrain softening can be resolved in a straightforward manner.

Figure 17 shows a hypothetical and schematic pole-to-pole cross section through the Martian regolith that appears to be broadly consistent with all the current data and theoretical considerations that bear on the issue of ground-ice distribution. The shaded region indicates the locations where ground ice is present. Ice extends very close to the surface at high latitudes. The top of the ground ice becomes deeper with decreasing latitude, dropping off fairly sharply in the vicinity of ± 30°. Ground ice is present at equatorial latitudes, but only at substantial depths. This ice distribution is in agreement with both theoretical considerations and observations of rampart craters.

The dashed line in Fig. 16 shows the depth at which the effective transition takes place from pulverized, thoroughly disaggregated debris near the surface to fractured bedrock below. The transition of course will be gradual

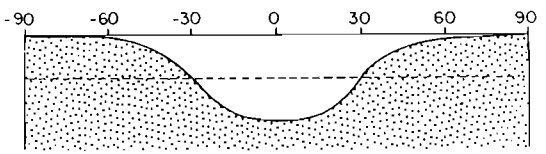

Fig. 17. Schematic representation of the distribution of ground ice in the Martian subsurface, as deduced from both terrain softening and rampart craters. Ice in the equatorial region has been removed to a substantial depth by sublimation and diffusion. Dashed line indicates the depth above which the crustal material has been sufficiently disaggregated by impacts that it is able to flow and produce terrain softening. Current understanding is inadequate to allow accurate labeling of the depth scale on the vertical axis.

rather than abrupt, but the effect on the mobility of materials will be qualitatively the same. Both materials are porous and can contain significant amounts of ice, but only the upper one has a structure that will allow creep deformation to occur. At latitudes higher than ± 30°, ice is present in near-surface, thoroughly disaggregated materials, and terrain softening can take place. At lower latitudes, ice only persists in deep, heavily fractured bedrock, still allowing rampart craters to form for large impacts, but preventing terrain softening. This picture is consistent with the observed distribution of ice-related features, with our knowledge of the rheology of ice-silicate mixtures, and with the expected vertical structure of the upper few km of the Martian surface. The vertical scale on Fig. 16 is left unlabeled intentionally. We do not know the depth to which terrain softening extends with any real accuracy; nor can we determine the depth to the top of the ice-rich layer with precision. It will be left to future investigations to fully characterize its regional variability and its quantitative details.

Despite the large uncertainties that still exist, a general picture has emerged of the subsurface distribution of ice on Mars that appears to be generally consistent with our understanding of the major physical processes involved. This general picture is certainly consistent with the view that H_2O has played a major role in the geologic evolution of the planet's surface. It may also have significant geophysical implications: the strong latitudinal dependences observed, coupled with the long time scales for migration of ground ice on Mars, may place severe constraints on hypotheses of significant polar wander on the planet. However, there is great potential for future investigation of ground ice on Mars. Techniques that could be applied, in order of increasing capability to probe to depth, include gamma-ray spectroscopy, direct sampling using penetrators or rover-mounted drills, electromagnetic sounding and seismology. All of these could contribute substantially to our understanding of the quantity of Martian ground ice, of its geographic distribution and of the physical processes that have controlled its evolution.

BIBLIOGRAPHY

Allen, C. C. 1978. Areal distribution of Martian rampart craters. *Icarus* 39:111-123.

Allen, C. C. 1979. Volcano-ice interactions on Mars. *J. Geophys. Res.* 84:8048-8059.

Andersland, O. B. and Akili, W. 1967. Stress effect on creep rates of a frozen clay soil. *Geotech.* 17:27-39.

Anderson, D. M. and Tice, A. R. 1973. The unfrozen interfacial phase in frozen soil water systems. In *Ecological Studies Analysis and Synthesis*, vol. 4, eds. A. Hadas, D. Swartzendruber, P. E. Rijtema, M. Fuchs and B. Yaron (New York: Springer-Verlag), pp.107-124.

Anderson, D. M., Gaffney, E. S., and Low, P. F. 1967. Frost phenomenon on Mars. *Science* 155: 319-322.

Baker, V. R. 1982. *The Channels of Mars* (Austin: Univ. of Texas Press).

Banin, A., and Anderson, D. M. 1974. Effects of salt concentration changes during freezing on the unfrozen water content of porous materials. *Water Resources Res.* 10:124-128.

Binder, A. B., and Lange, M. A. 1980. On the thermal history of a moon of fission origin. *J. Geophys. Res.* 85:3194-3208.

Boyce, J. M. 1980. Distribution of thermal gradient values in the equatorial region of Mars based on impact crater morphology. In *Reports of Planetary Geology Program-1980*, NASA TM-82385, pp. 140-143.

Brace, W. F. 1980. Permeability of crystalline and argillaceous rocks. *Intl. J. Rock Mech. Mining Sci. Geochem. Abst.* 17:241-251.

Brace, W. F. 1984. Permeability of cystalline rocks: New in situ measurements. *J. Geophys. Res.* 89:4327-4330.

Brass, G. W. 1980. Stability of brines on Mars. *Icarus* 42:20-28.

Byerlee, J. D., and Brace, W. F. 1968. Stick-slip, stable sliding, and earthquakes-Effect of rock type, pressure, strain rate, and stiffness. *J. Geophys. Res.* 73:6031-6037.

Carr, M. H. 1979. Formation of Martian flood features by release of water from confined aquifers. *J. Geophys. Res.* 84:2995-3007.

Carr, M. H. 1986. Mars: A water-rich planet? *Icarus* 56:187-216.

Carr, M. H., and Schaber, G. G. 1977. Martian permafrost features. *J. Geophys. Res.* 82:4039-4054.

Carr, M. H., Crumpler, L. S., Cutts, J. A., Greeley, R., Guest, J. E., and Masursky, H. 1977b. Martian impact craters and emplacement of ejecta by surface flow. *J. Geophys. Res.* 82:4055-4065.

Chapman, C. R., and McKinnon, W. B. 1986. Cratering of planetary satellites. In *Satellites*, eds. J. A. Burns and M. S. Matthews (Tucson: Univ. of Arizona Press), pp.492-580.

Clark, B. C. 1978. Implications of abundant hygyroscopic minerals in the Martian regolith. *Icarus* 34:645-665.

Clark, B. C., and Van Hart, D. C. 1981. The salt of Mars. *Icarus* 45:370-378.

Clark, B. C., Baird, A. K., Rose, H. J., Toulmin, P., III, Keil, K., Castro, A. J., Kelliher, W. C., Rowe, C. D., and Evans, P. H. 1976. Inorganic analysis of Martian surface samples at the Viking landing sites. *Science* 194:1283-1288.

Clifford, S. M. 1984. A Model for the Climatic Behavior of Water of Mars. Ph.D. Thesis, Univ. of Massachusetts.

Clifford, S. M. 1987b. Polar basal melting on Mars. *J. Geophys. Res.* 92:9135-9152.

Clifford, S. M., and Fanale, F. P. 1985. The thermal conductivity of the Martian dust. *Proc. Lunar Planet. Sci. Conf.* 16, *J. Geophys. Res. Suppl.* 90:D144-D145.

Clifford, S. M., and Hillel, D. 1983. The stability of ground ice in the equatorial regions of Mars. *J. Geophys. Res.* 88:2456-2474.

Costard, F. M. 1987. Quelques modeles lies a des lentilles de glace fossiles sur Mars. *Zeit. Geomorph.* 31:243-251.

Costard, F. M. 1988. Thickness of sedimentary deposits of the mouth of outflow channels. *Lunar Planet. Sci.* XIX:211-212.

Costard, F. M. 1989. Asymmetric distribution of volatiles on Mars. *Lunar Planet. Sci.* XX:187-188 (abstract).

BIBLIOGRAPHY

Costard, F., and Dollfus, A. 1987. Ice lenses on Mars. In *MECA Special Section at LPSC XVII: Martian Geomorphology and Its Relation to Subsurface Volatiles*, eds. S. M. Clifford, L. A. Rossbacher and J. R. Zimbelman, LPI Tech. Rept. 87-02, pp. 16-17 (abstract)

Crescenti, G. H. 1984. Analysis of permafrost depths on Mars. In, NASA TM 86247, pp. 115-132.

Croft, S. K. 1980. Cratering flow field; Implications for the excavation and transient expansion stages of crater formation. *Proc. Lunar Planet. Sci. Conf.* 11:2347-2378.

Croft, S. K. 1984. Scaling of complex craters. *Lunar Planet. Sci.* XV:188-189 (abstract).

Croft, S. K., Kieffer, S. W., and Ahrens, T. J. 1979. Low-velocity impact craters in ice-saturated sand with implications for Martian crater count ages. *Proc. Lunar Planet. Sci. Conf.* 14, *J. Geophys. Res. Suppl.* 89:B8023-B8032.

Czudek, T., and Demek, J. 1970. Thermokarst in Siberia and its influence on the development of lowland relief. *Quat. Res.* 1:103-120.

Davies, G. F., and Arvidson, R. E. 1981. Martian thermal history, core segregation, and tectonics. *Icarus* 45:339-346.

Davis, B. W. 1969. Some speculations on absorption and desorption of CO_2 in martian bright regions. *Icarus* 11:155-158.

de Marsily, G., Ledoux, E., Barbraeu, A., and Margat, J. 1977. Nuclear waste disposal: Can the geologists guarantee isolation? *Science* 197:519-527.

Dence, M. R., Grieve, R. A. F., and Robertson, P. B. 1977. Terrestrial impact structures: Principal characteristics and energy considerations. In *Impact and Explosion Cratering*, eds. D. J. Roddy, R. O. Pepin and R. B. Merrill (New York: Pergamon), pp. 247-276.

Ersoy, T., and Togro, E. 1978. Temperature and strain rate effects on the strength of compacted frozen silt-clay. In *Third Intl. Conf. on Permafrost*, pp. 643-647.

Evans, N., and Rossbacher, L. A. 1980. The last picture show: Small-scale patterned ground in Lunae Planum. In *Reports of Planetary Geology Program-1980*, NASA TM-82385, pp. 376-378.

Fanale, F. P. 1976. Martian volatiles: Their degassing history and geochemical fate. *Icarus* 28: 179-202.

Fanale, F. P., Salvail, J. R., Zent, A. P., and Postawko, S. E. 1986. Global distribution and migration of subsurface ice on Mars. *Icarus* 67:1-18.

Farmer, C. B., and Doms, P. E. 1979. Global and seasonal variation of water vapor on Mars and the implications for permafrost. *J. Geophys. Res.* 84:2881-2888.

Fetter, C. W. 1980. *Applied Hydrogeology* (Columbus, Ohio: C. E. Merrill).

Frey, H. V., Lowry, B. L., and Chase, S. A. 1979. Pseudocraters on Mars. *J. Geophys. Res.* 84: 8075-8086.

Gault, D. E., and Greeley, R. 1978. Exploratory experiments of impact craters formed in viscous-liquid targets: Analogs for Martian rampart craters? *Icarus* 33:483-513.

Gooding, J. L. 1978. Chemical weathering on Mars: Thermodynamic stabilities of primary minerals (and their alteration products) from mafic igneous rocks. *Icarus* 33;483-513.

Greeley, R., and Spudis, P. 1981. Volcanism on Mars. *Rev. Geophys. Space Phys.* 19:13-41.

Grizzaffi, P., and Schultz, P. H. 1989. Isidis basin: Site of ancient volatile-rich debris layer. *Icarus* 77:358-381.

Gurnis, M. 1981. Martian cratering revisited: Implications for early geologic evolution. *Icarus* 48: 62-75.

Haynes, D. F. 1978. Strength and deformation of frozen silt. In *Third Intl. Conf. on Permafrost*, pp. 656-661.

Hartmann, W. K. 1973a. Ancient lunar mega-regolith and subsurface structure. *Icarus* 18:634-636.

Hartmann, W. K. 1980. Dropping stones in magma oceans: Effects of early lunar cratering. In *Proc. Conf. on the Lunar Highlands Crust*, eds. J. J. Papike and R. B. Merrill (New York: Pergamon), pp. 155-171.

Hobbs, P. V. 1974. *Ice Physics* (London; Oxford Univ. Press).

Hodges, C. A., and Moore, H. J. 1979. The subglacial birth of Olympus Mons and its aureoles. *J. Geophys. Res.* 84:8061-8074.

Horner, V. M., and Barlow, N. G. 1988. Martian craters: Changes in the diameter range for ejecta fluidization with latitude. *Lunar Planet. Sci.* XIX:505-506 (abstract).

Hubert, M. K., and Rubey, W. W. 1959. Role of fluid pressure in mechanics of overthrust faulting. *Bull. Geol. Soc. Amer.* 70:115.

Huguenin, R. L. 1976. Mars: Chemical weathering as a massive volatile sink. *Icarus* 28:203-212.

Ivanov, B. A. 1986. *Cratering Mechanics*, NASA TM-88477 (N87-15662).

Ivanov, B. A. 1988a. Effect of modification of impact craters on the size-frequency distribution and scaling law. *Lunar Planet. Sci.* XIX:531-532 (abstract).

Ives, R. L. 1940. Rock glaciers in the Colorado Front Range. *Bull. Geol. Soc. Amer.* 51:1271-1294.

Jones, J. G. 1970. Intraglacial volcanoes of the Laugarvatn region, southwest Iceland. *J. Geol.* 78:127-140.

Kahn, R. 1985. The evolution of CO_2 on Mars. *Icarus* 62:175-190.

Kahn, R., Guinness, E. A., Arvidson, R. E. 1986. Loss of fine-scale surface texture in the Viking Orbiter images and implications for the inferred distribution of debris mantles. *Icarus* 66:2-38.

Kieffer, H. H. 1976. Soil and surface temperatures at the Viking Lander sites. *Science* 194:1344-1346.

Kieffer, S. W., and Ahrens, T. J. 1980. The role of volatiles and lithology in the impact cratering process. *Rev. Geophys. Space Phys.* 18:143-181.

Kuzmin, R. O. 1977. Questions of the structure of the Martian cryolithosphere. In *Problems of Cryolithology*, vol. 6 (Moscow: Univ. Press), p. 7-25.

Kuzmin, R. O. 1978. The peculiarities of the Martian cryolithosphere and its display in relief. In *Problems of Cryolithology*, vol. 7 (Moscow: Univ. Press), p.7-27.

Kuzmin, R. O. 1980a. Determination of the bedding depth of ice rocks on Mars from the morphology of fresh craters. *Dokl. ANSSSP* 252:1445-1448.

Kuzmin, R. O. 1983. *Cryolithosphere of Mars.* (Izdatel'stvo Nauka).

Kuzmin, R. O., Bobina, N. N., Zabalueva, E. V., and Shashkina, V. P. 1988b. Structure inhomogeneities of the Martian cryolithosphere. *Solar System Res.* 22:195-212.

Kuzmin, R. O., Bobina, N. N., Zabalueva, E. V., and Shashkina, V. P. 1989. Martian cryolithosphere: Structure and relative ice content. *Intl. Geol. Congress*, in press (abstract).

Legrand, H. 1979. Evaluation techniques of fractured-rock hydrology. *J. Hydrology*, p. 333-346.

Lucchitta, B. K. 1981. Mars and Earth: Comparison of cold-climate features. *Icarus* 45:264-303.

Lucchitta, B. K. 1983a. Ice lubricated flow in Martian fretted channels and implications for outflow channel processes. *Proc. Lunar Planet. Sci. Conf.* 14, *J. Geophys. Res. Suppl.* 89:B446-B447.

Lucchitta, B. K. 1983b. Permafrost on Mars: Polygonally fractured ground. In *Permafrost: Proc. Fourth Intl. Conf. Proc.* July 17-22, Fairbanks, Al. (Washington, D.C.: National Academy Press), pp. 744-749.

Lucchitta, B. K. 1984a. Ice and debris in the fretted terrain, Mars. *Proc. Lunar Planet. Sci. Conf.* 14, *J. Geophys. Res. Suppl.* 89:B409-B418.

Lucchitta, B. K. 1985a. Geomorphologic evidence for ground ice on Mars. In *Ices in the Solar System*, eds. J. Klinger, D. Benest, A. Dolfus and R. Smoluchowski (New York: D. Reidel), pp.585-604.

Lucchitta, B. K. 1985b. Valles Marineris basin beds: A complex story. In *Reports of Planetary Geology Program* 1984, NASA TM-87563, p. 506-508 (abstract).

Lucchitta, B. K. 1987c. Valles Marineris, Mars: Wet debris flows and ground ice. *Icarus* 72:411-429.

Lucchitta, B. K., and Ferguson, H. M. 1983. Chryse Basin channels: Low gradients and ponded flows. *Proc. Lunar Planet. Sci. Conf.* 13, *J. Geophys. Res. Suppl.* 88:A553-A568.

Lucchitta, B. K., Ferguson, H. M., and Summers, C. 1986. Sedimentary deposits in the northern lowland plains, Mars. *Proc. Lunar Planet. Sci. Conf.* 17, *J. Geophys. Res. Suppl.* 91:E166-E174.

Malin, N. C. 1974. Salt weathering on Mars. *J. Geophys. Res.* 79:3888-3894.

Maxwell, J. C. 1964. Influence of depth, temperature, and geologic age on the porosity of quartzose sandstone. *Bull. Amer. Assoc. Petrol. Geol.* 48:697-709.

McGill, G. E. 1986. The giant polygons of Utopia, northern Martian plains. *Geophys. Res. Lett.* 13:705-708.

Melosh, H. J. 1980a. Cratering mechanics-Observational, experimental, and theoretical. *Ann. Rev. Earth Planet. Sci.* 8:65-93.

Melosh, H. J. 1989. *Impact Cratering. A Geologic Process* (New York:Oxford Univ. Press).

Mouginis-Mark, P. J. 1979. Martian fluidized crater morphology: Variations with crater size, latitude, altitude, and target material. *J. Geophys. Res.* 84:8011-8022.

O'Keefe, J. D., and Ahrens, T. J. 1981. Impact cratering: The effect of crustal strength and planetary gravity. *Rev. Geophys. Space Phys.* 19:1-12.

Pechmann, J. C. 1980. The origin of polygonal troughs on the northern plains of Mars. *Icarus* 42: 185-210.

Penner, E. 1970. Thermal conductivity of frozen soils. *Canadian J. Earth Sci.* 7:982-987.

Pettijohn, F. L. 1975. *Sedimentary Rocks*, 3rd ed. (New York: Harper and Row).

Phukan, A. 1983. Long-term creep deformation of roadway embankment on ice-rich permafrost. In *Proc. Fourth Intl. Conf. on Permafrost*, July 17-22, Fairbanks, Alaska (Washington, D.C.: National Academy Pres), pp. 994-999.

Pollack, J. B., Kasting, J. F., Richardson, S. M., and Poliakof, K. 1987. The case for a wet, warm climate on early Mars. *Icarus* 71:203-224.

Postawko, S. E., and Kuhn, W. R. 1986. Effect of the grenhouse gases (CO_2, H_2O, SO_2) on Martian paleoclimate. *Proc. Lunar Planet. Sci. Conf.* 16, *J. Geophys. Res. Suppl.* 91:D431-D438.

Ratcliffe, E. H. 1962. The thermal conductivity of ice: New data on the temperature coefficient. *Phil. Magnet.* 1:1197-1203.

Rittenhouse, G. 1971. Pore-space reduction by solution and cementation. *Amer. Assoc. Petrol. Geol. Bull.* 55:80-91.

Rossbacher, L. A., and Judson, S. 1981. Ground ice on Mars: Inventory, distribution, and resulting landforms. *Icarus* 45:39-59.

Sadovsky, A. V., and Bondarenko, G. I. 1983. Creep of frozen soils on rock slopes. In *Proc. Fourth Intl. Conf. on Permafrost*, pp.1101-1104.

Schultz, P. H. 1986. Crater ejecta morphology and the presence of water on Mars. *In Symp. on Mars: Evolution of its Climate and Atmosphere*, LPI Contrib. 599 (Houston: Lunar and Planetary Inst.), pp.95-97.

Schultz, P. H., and Gault, D. E. 1979. Atmospheric effects on Martian ejecta emplacement. *J. Geophys. Res.* 84:7669-7687.

Seeburger, D. A., and Zoback, M. D. 1982. The distribution of natural fractures and joints at depth in cystalline rock. *J. Geophys. Res.* 87:5517-5534.

Sharp, R. P. 1973a. Mars: Fretted and chaotic terrain. *J. Geophys. Res.* 78:4073-4083.

Shoemaker, E. M. 1963. Impact mechanics at Meteor Crater, Arizona. In *The Moon, Meteorites, and Comets*, eds. B. M. Middlehurst and G. P. Kuiper (Chicago: Univ. of Chicago Press), pp. 301-336.

Shoji, H., and Higashi, A. 1978. A deformation mechanism map of ice. *J. Glaciol.* 21:419-427.

Short, N. M. 1970. Anatomy of a meteorite impact crater: West Hawk Lake, Manitoba, Canada. *Geol. Soc. Amer. Bull.* 81:609-648.

Smoluchowski, R. 1968. Mars: Retention of ice. *Science* 159:1348-1350.

Soderblom, L. A., Condit, C. D., West, R. A., Herman, B. M., and Kriedler, T. J. 1974. Martian planetwide crater distributions: Implications for geologic history and surface processes. *Icarus* 22:239-263.

Soderblom, L. A., Malin, M. C., Cutts, J. A., and Murray, B. C. 1973b. Mariner 9 observations of the surface of Mars in the north polar region. *J. Geophys. Res.* 78:4197-4210.

Soloviev, P. A. 1973. Thermokarst phenomena and landforms due to frost heaving in central Yakutia. *Biuletyn Peryglacjalny* 23:135-155.

Squyres, S. W. 1978. Martian fretted terrain: Flow of erosional debris. 34:600-613.

Squyres, S. W. 1979a. The distribution of lobate debris aprons and similiar flows on Mars. *J. Geophys. Res.* 84:8087-8096.

BIBLIOGRAPHY

Squyres, S. W. 1984. The history of water on Mars. *Ann. Rev. Earth Planet. Sci.* 12:83-106.

Squyres, S. W. 1989c. Urey prize lecture: Water on Mars. *Icarus* 79:229-288.

Squyres, S. W., and Carr, M. H. 1986. Geomorphic evidence for the distribution of ground ice on Mars. *Science* 231:249-252.

Stoffler, D., Gault, F. E., Wedekind, J., and Polkowski, G. 1975. Experimental hypervelocity impact into quartz sand: Distribution and shock metamorphism of ejecta. *J. Geophys. Res.* 80: 4062-4077.

Streltsova, T. D. 1976. Hydrodynamics of groundwater flow in a fractured formation. *Water Resources Res.* 12:405-414.

Theilig, E., and Greeley, R. 1979. Plains and channels in the Lunae Planum-Chryse Planitia region of Mars. *J. Geophys. Res.* 4:7994-8010.

Thompson, E. G., and Sayles, F. H. 1972. In situ creep analysis of room in frozen soil. *J. Soil Mech.* 98:899-915.

Thompson, W. F. 1962. Preliminary notes on the nature and distribution of rock glaciers relative to true glaciers and other effects of the climate on the ground in North America. *In Symp. at Obergurgl.* Intl. Asoc. Sci. Hydrol. Publ. No. 58 (Obergurgl: Intl. Asoc. Sci. Hydrology), pp. 212-219.

Thorarinsson, S. 1953. The crater group in Iceland. *Bull. Vol. Ser.* 2 14:3-44.

Toksoz, N. M. 1979. Planetary seismology and interiors. *Rev. Geophys. Space Phys.* 17:1641-1655.

Toksoz, N. M., and Hsui, A. T. 1978. Thermal history and evolution of Mars. *Icarus* 34:537-547.

Toon, O. B., Polack, J. B., Wrd, W., Burns, J. A., and Bilski, K. 1980. The astronomical theory of climatic change on Mars. *Icarus* 4:552-607.

Toulmin, P., Baird, A. K., Clark, B. C., Keil, K., Rose, H. J., Jr., Christian, R. P., Evans, P. H., and Kelliher, W. C. 1977. Geochemical and mineralogical interpretation of the Viking inorganic chemical results. *J. Geophys. Res.* 84:4625-4634.

Wahrhaftig, C., and Cox, A. 1959. Rock glaciers in the Alaska Range. *Bull. Geol. Soc. Amer.* 70: 383-436.

Ward, W. R. 1979. Present obliquity oscilations of Mars: Fourth-order accuracy in orbital e and I. *J. Geophys. Res.* 84:237-241.

Warren, P. H., and Rasmussen, K. L. 1987. Megaregolith insulation, internal temperatures, and the bulk uranium content of the Moon. *J. Geophys. Res.* 92:3453-3465.

Washburn, A. L. 1973. *Periglacial Processes and Environments* (New York: St. Martin's).

Weerdenburg, P.C., and Morgenstern, N. R. 1983. Underground cavities in ice-rich frozen ground. In *Permafrost: Proc. Fourth Intl Confer.*, July 17-22, Fairbanks, Alaska. (Washington, D. C.: National Academy Press), pp. 1384-1389.

White, S. E. 1976. Rock glaciers and block fields, review and new data. *Quat. Res.* 6:77-97.

Zimbelman, J. R., Clifford, A. M., and Williams, S. H. 1989. Concentric crater fill on Mars: An aeolian alternative to ice-rich mass wasting. *Proc. Lunar Planet. Sci. Conf.* 19:397-407.